Soil Dynamics and Earthquake Engineering 113 (2018) 545–571

Contents lists available at ScienceDirect

Soil Dynamics and Earthquake Engineering

journal homepage: www.elsevier.com/locate/soildyn

Bridges crossing fault rupture zones: A review

Shuo Yang, George P. Mavroeidis*

Department of Civil and Environmental Engineering and Earth Sciences, University of Notre Dame, Notre Dame, IN 46556, USA

ARTICLE INFO

Keywords:
Case study
Fault rupture zone
Fault-crossing bridge
Experimental investigation
Simplified analysis
Numerical analysis
Response history analysis
Seismic design code

ABSTRACT

Several earthquakes over the past two decades have demonstrated that bridges crossing fault rupture zones may suffer significant damage due to the combined effects of ground shaking and surface rupture. Although it is widely recommended to avoid building a bridge across a fault, it is not always possible to achieve this objective, especially in regions with a dense network of active faults. This review begins by compiling two databases: one of fault-crossing bridges damaged in past earthquakes and another of bridges crossing potentially active fault rupture zones. The article then continues to review findings of experimental, analytical and numerical studies, and to summarize seismic design provisions and recommendations related to fault-crossing bridges. The review ends with suggestions for future research directions in this area.

1. Introduction

The vulnerability of bridges crossing active fault rupture zones (called "fault-crossing bridges" in this study) has received increasing attention from earthquake engineers over the past two decades. The impetus was provided by the devastating effects of the 1999 M_w 7.4 Kocaeli, 1999 M_w 7.6 Chi-Chi, and 1999 M_w 7.2 Duzce earthquakes on bridge structures traversed by fault rupture zones. Although it is widely recommended to avoid building a bridge across a fault, it is not always possible to achieve this objective, especially in regions with a dense network of active faults.

Active faults that break through the ground surface and have the potential to generate significant fault offset in the event of an earthquake have the capacity to impose a severe combination of ground shaking and surface rupture on fault-crossing bridges. In general, the fault offset may vary from a few centimeters to several meters depending on the earthquake magnitude (e.g., [133]). Similar to non-fault-crossing bridges located in the vicinity of a fault, fault-crossing bridges are subjected to near-fault-pulse-like ground motions affected by forward directivity and permanent translation (fling) (e.g., [81]), but now these ground motions vary across the fault rupture.

According to Slemmons and dePolo [111], there are three main types of surface rupture associated with faulting (Fig. 1): (1) primary rupture, which occurs along the primary fault where most of the seismic energy is released; (2) secondary rupture, which occurs along a secondary (or branch) fault subordinate to the primary fault; and (3) sympathetic (or triggered) rupture, which occurs along another nearby fault that is disturbed by the strain release along the primary fault or the vibratory ground motion. It is noted that a surface fault rupture should not be viewed as a fault line, but rather as a fault zone with a finite width subjected to ground distortion. In this study, a fault-crossing bridge is defined as a bridge structure traversed by a surface fault rupture zone (primary, secondary or sympathetic) passing beneath any portion of the bridge (span, pier, abutment or approach road) (Fig. 1).

This article presents a comprehensive review of case studies, experimental, analytical and numerical investigations, and seismic design codes related to fault-crossing bridges. Two databases – one of fault-crossing bridges damaged in past earthquakes and another of bridges crossing potentially active fault rupture zones – are first compiled based on information provided in the literature. Findings of experimental, analytical and numerical studies of bridges traversed by fault rupture zones are then reviewed. Seismic design provisions and recommendations related to fault-crossing bridges are also summarized. Finally, suggestions for future research directions in this area are proposed. It is noted that a review of studies focusing on other types of structures (e.g., tunnels, dams, pipelines, buildings, etc.) crossing fault rupture zones is beyond the scope of this article.

2. Fault-crossing bridges damaged in past earthquakes

In this section, detailed information about fault-crossing bridges that were damaged in past earthquakes is collected from the literature. This information, which is summarized in Table 1 and discussed next, includes description of bridges, damaging earthquakes, fault crossing conditions and observed damage modes, as well as a comprehensive list

* Corresponding author.
E-mail address: g.mavroeidis@nd.edu (G.P. Mavroeidis).

https://doi.org/10.1016/j.soildyn.2018.03.027
Received 2 February 2018; Received in revised form 17 March 2018; Accepted 20 March 2018

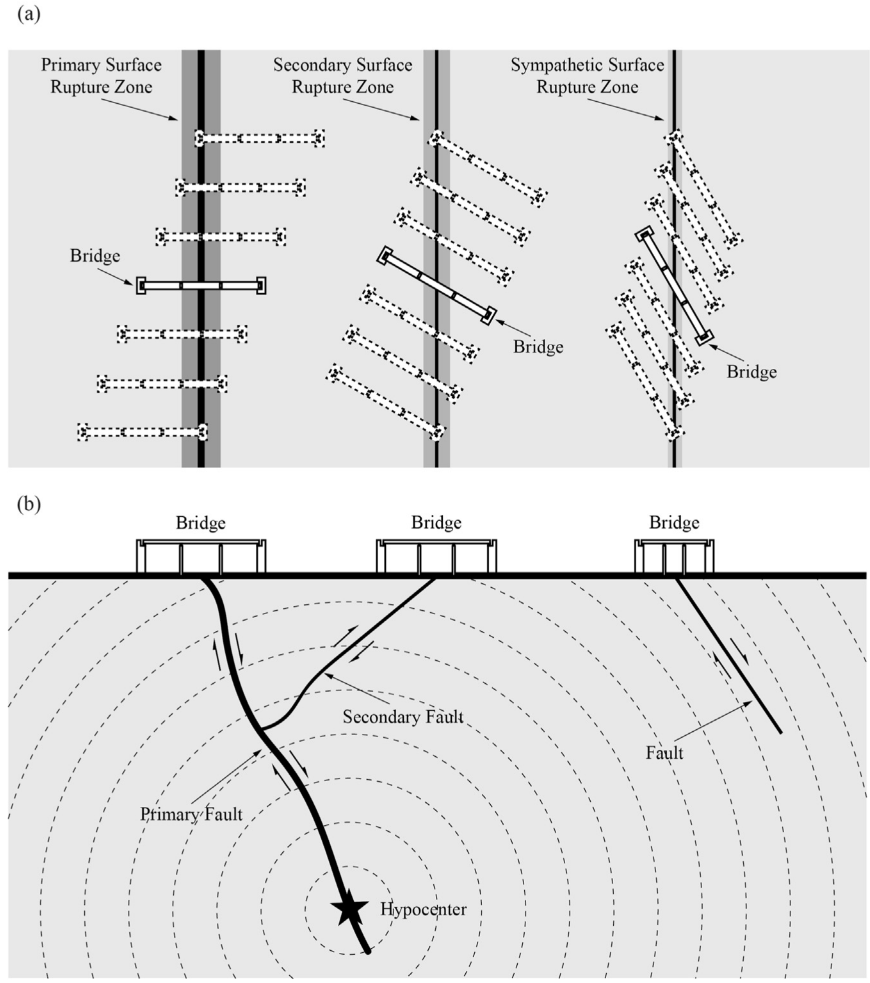

Fig. 1. Schematic of bridges crossing surface fault rupture zones: (a) plan view showing different fault crossing angles and locations; (b) cross-section showing different types of fault rupture (primary, secondary, and sympathetic).

of references.[1] This survey builds upon earlier review studies on this subject conducted by Kawashima [61,62] and Hui [53].

2.1. The 1906 M_w 7.8 San Francisco, California, earthquake

The earliest seismic event associated with damage to bridges induced by surface fault rupture appears to be the 1906 San Francisco earthquake. Specifically, a bridge spanning the Alder Creek northwest from Point Arena was severely damaged when the fault trace passed beneath the bridge near its southwest abutment (Fig. 2a), resulting in the collapse of the Alder Creek Bridge (Fig. 2b) [70]. The horizontal offset along the fault trace, which was greater than the width of the bridge, is also shown in Fig. 2b. A railway bridge spanning the Pajaro River at Chittenden was also damaged due to fault crossing during the 1906 San Francisco earthquake [70,120,10]. The Pajaro River Bridge was a 5-span, curved, steel truss bridge supported by wall-type piers (Fig. 3a and c). The fault trace crossed the bridge beneath pier P3 at an angle of approximately 45° with respect to the bridge axis (Fig. 3c), leading to cracking and displacement of the supporting piers. In addition, as illustrated in Fig. 3b and c, the bridge was dragged from abutment A2 (west abutment) about 1.1 m (3.5 ft), thus lengthening the distance between the abutments. Finally, as mentioned in passing by Lawson et al. [70], two additional bridges – a rough wooden bridge spanning the South Fork of the Gualala River and an old bridge spanning the Russian River – were severely damaged due to fault crossing during the 1906 San Francisco earthquake, but are not discussed further herein due to insufficient information.

2.2. The 1999 M_w 7.4 Kocaeli (Izmit), Turkey, earthquake

The Arifiye Overpass (No. 3 Overpass), located on the Trans-European Motorway near the city of Adapazari, was a 104-m-long, 4-span, skewed, simply-supported, prestressed concrete U-beam bridge (Fig. 4a) on wall-type piers (Fig. 4b) and seat-type abutments (Fig. 4c). Each pier or abutment was supported on cast-in-place reinforced concrete piles (e.g., [56,38,61,62,26,97,138]). The fault rupture zone of the 1999 Kocaeli earthquake passed between abutment A1 (northeast abutment) and pier P1 at an angle of approximately 65° with respect to the longitudinal axis of the bridge (e.g., [126,7]). As shown in Fig. 4d, the northernmost span completely collapsed, whereas the remaining three spans fell off their supports causing 10 fatalities among the passengers of a passing bus [26].

The No. 1 Overpass, located about 1 km east of the Arifiye Overpass, was a 2-span, simply-supported, prestressed concrete bridge on wall-type piers. The bridge was crossed through its southeast abutment by the fault rupture zone of the 1999 Kocaeli earthquake (Fig. 5a) causing a 50-mm shear deformation in the elastomeric bearings and minor damage overall (Fig. 5b) (e.g., [61,62,26,53]). The No. 2 Overpass,

[1] A few additional cases of fault-crossing bridges damaged in past earthquakes have been reported in the literature, but are neither listed in Table 1 nor discussed in this section due to insufficient information or knowledge of the language in which the relevant references are published. This includes two fault-crossing bridges damaged during the recent 2016 M_w 7.0 Kumamoto, Japan, earthquake [109,90,118].

Table 1
Fault-crossing bridges damaged in past earthquakes.

Bridge name	Location	Year of completion[a]	Total length (m)[b]	Number of spans	Inter-span relationship[c]	Girder[d]	Pier[e]
1906 M_w 7.8 San Francisco, California, earthquake							
Alder Creek Bridge	USA	N/A	N/A	N/A	N/A	N/A	N/A
Pajaro River Bridge	USA	N/A	N/A	5	N/A	Steel truss	WTP
1999 M_w 7.4 Kocaeli (Izmit), Turkey, earthquake							
Arifiye Overpass	Turkey	1991	104	4	SS	PC U-girder	WTP
No. 1 Overpass	Turkey	N/A	N/A	2	SS	N/A	WTP
No. 2 Overpass	Turkey	N/A	N/A	4	SS	N/A	WTP
No. 4 Overpass	Turkey	N/A	N/A	4	SS	N/A	WTP
Sakarya Center Bridge	Turkey	N/A	92	8	SS	N/A	CPP
1999 M_w 7.6 Chi-Chi, Taiwan, earthquake							
Pi-Feng Bridge	Taiwan	1991	325	13	SS	PC I-girder	SCP
Wu-Shi Bridge	Taiwan	1981 & 1983	625	18	SS	PC I-girder	SCP &WTP
Shi-Wei Bridge	Taiwan	1994	75	3	SS	PC I-girder	SCP
E-Jian Bridge	Taiwan	1972	264	24	SS	PC double-T-girder	WTP
Ming-Tsu Bridge	Taiwan	1990	700	28	SS	PC I-girder	SCP
Tong-Tou Bridge	Taiwan	1980	160	4	SS	PC I-girder	SCP
Chang-Geng Bridge	Taiwan	1987	408	13	SS	PC I-girder	SCP
Bauweishan Bridge	Taiwan	(1999)	N/A	5	SS	N/A	N/A
Pinlinchi Bridge	Taiwan	(1999)	N/A	11	N/A	N/A	N/A
Minchien Viaduct	Taiwan	(1999)	N/A	N/A	N/A	N/A	N/A
1999 M_w 7.2 Duzce, Turkey, earthquake							
Bolu Viaduct 1	Turkey	(1999)	2300	59	SS	PC box-girder	SCP
2008 M_w 7.9 Wenchuan, China, earthquake							
Gaoshu Bridge	China	(2008)	248	18	SS	RC hollow-slab	SCP & DCP
Xiaoyudong Bridge	China	1999	189	4	SS	RC rigid-frame arch	DCP

Bridge name	Foundation[f]	Bearing[g]	Fault name	Fault type[h]	Fault crossing angle (°)	Fault crossing location[i]	Damage mode[j]	Reference
1906 M_w 7.8 San Francisco, California, earthquake								
Alder Creek Bridge	N/A	N/A	San Andreas	SS	~ 90	Near A2	Collapse	[70]
Pajaro River Bridge	N/A	N/A	San Andreas	SS	~ 45	P3	Significant	[10,70,120]
1999 M_w 7.4 Kocaeli (Izmit), Turkey, earthquake								
Arifiye Overpass	PF	EB	North Anatolian	SS	~ 65	A1-P1	Collapse	[5,7,26,38,49,53,54,5-6,61,62,87,97,105,12-5,126,138]
No. 1 Overpass	N/A	EB	North Anatolian	SS	N/A	A2	Repairable	[26,53,54,61,62]
No. 2 Overpass	N/A	EB	North Anatolian	SS	N/A	A1	Repairable	[26,53,54,61,62]
No. 4 Overpass	N/A	EB	North Anatolian	SS	N/A	A2	Repairable	[26,53,54,61,62]
Sakarya Center Bridge	N/A	N/A	North Anatolian	SS	N/A	A1	Collapse	[26,53,61,62,105,126]
1999 M_w 7.6 Chi-Chi, Taiwan, earthquake								
Pi-Feng Bridge	CF	EB	Chelungpu	RV	~ 20–40	A2-P11	Collapse	[2,5,7,12,15,21,23,30,-34,53,54,61,62,64,66,-73,74,88,93,97,117,1-28,129,139,142,144]
Wu-Shi Bridge	CF	EB	Chelungpu	RV	~ 40	P2-P3	Collapse	[2,5,12,15,21,23,34,5-0,53,54,61,62,64,65,7-3,74,88,93,117,127–1-29,139,142,144]
Shi-Wei Bridge	CF	EB	Chelungpu	RV	N/A	Near A2	Collapse	[2,15,21,23,53,54,69,-74,93,97,117,128,129-,139,142,144]

Table 1 (*continued*)

Bridge name	Foundation[f]	Bearing[g]	Fault name	Fault type[h]	Fault crossing angle (°)	Fault crossing location[i]	Damage mode[j]	Reference
E-Jian Bridge	SFF	NB	Chelungpu	RV	~ 50	Near A2 & P1-P2	Collapse	[2,15,21,34,66,73,74,-88,93,117,128,129,13-9,142]
Ming-Tsu Bridge	CF	EB	Chelungpu	RV	N/A	Near A2	Collapse	[2,15,21,53,54,73,74,-93,117,128,129,139,1-42]
Tong-Tou Bridge	CF	EB	Chelungpu	RV	N/A	Near A1	Collapse	[2,15,21,53,54,73,74,-93,117,128,129,139,1-42,144]
Chang-Geng Bridge	CF	EB	Chelungpu	RV	N/A	Near A1 & A2	Collapse	[2,12,15,21,53,54,74,-93,117,119,128,129,1-39,142]
Bauweishan Bridge	PF	N/A	Chelungpu	RV	N/A	P1	Significant	[22,66]
Pinlinchi Bridge	PF & SFF	N/A	Chelungpu	RV	N/A	P10	Significant	[22]
Minchien Viaduct	PF	N/A	Chelungpu	RV	N/A	A1	Significant	[22]
1999 M_w 7.2 Duzce, Turkey, earthquake								
Bolu Viaduct 1	PF	PB	North Anatolian	SS	~ 20–30	P44S-P45S & P46N-P47N	Significant	[5,12,26,30,31,36,37,-45,53,54,56,58,61,62,-78,89,97,98,100,101,-124–126]
2008 M_w 7.9 Wenchuan, China, earthquake								
Gaoshu Bridge	PF	EB	Longmenshan	RV	~ 90	P8-P9	Collapse	[53,54,71,82,130,132,-145,147,149,152]
Xiaoyudong Bridge	PF	EB	Longmenshan	RV	~ 75	Approach road behind A1	Collapse	[8,32,46,52–54,63,68,-71,72,75,107,108,116-,130,131,146,147,14-9–152]

Note: N/A = not available.

[a] Year in parentheses indicates that bridge was under construction when earthquake occurred. Years of completion for east and west bridges of Wu-Shi Bridge were 1981 and 1983, respectively.

[b] Approximate length based on information provided in the literature.

[c] SS, simply-supported.

[d] PC, prestressed concrete; RC, reinforced concrete.

[e] WTP, wall-type pier; CPP, capped pile pier; SCP, single-column pier; DCP, double-column pier.

[f] PF, pile foundation; CF, caisson foundation; SFF, spread footing foundation.

[g] EB, elastomeric bearing; PB, pot bearing; NB, no bearing.

[h] SS, strike-slip; RV, reverse.

[i] Fault crossing locations for Bauweishan Bridge, Pinlinchi Bridge, and Minchien Viaduct are shown in figure 3, figure 4, and photo 3 of Chen et al. [22], respectively. Fault crossing locations for all other bridges are shown in Figs. 2–15.

[j] Damage has been classified into five categories based on the criteria proposed by Erdik et al. [26] for non-fault-crossing bridges: None, no observable sign of earthquake-related distress; Minimal, members remain functional after a major seismic event without requiring repair; Repairable, damage can be repaired without threatening the bridge's overall functionality; Significant, damage may cause bridge closure or instability; Collapse, partial or total collapse of the bridge.

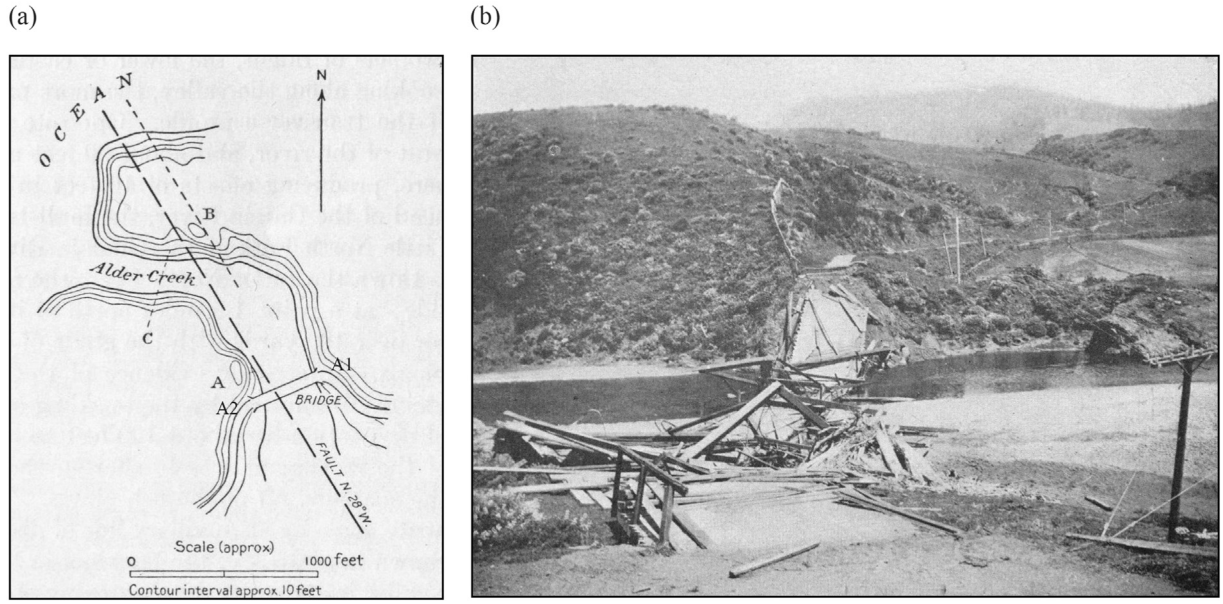

Fig. 2. Alder Creek Bridge during the 1906 San Francisco earthquake: (a) fault trace crossing bridge; (b) collapsed bridge (Fig. 2a is modified from Lawson et al. [70]; Fig. 2b is reprinted from Lawson et al. [70]).

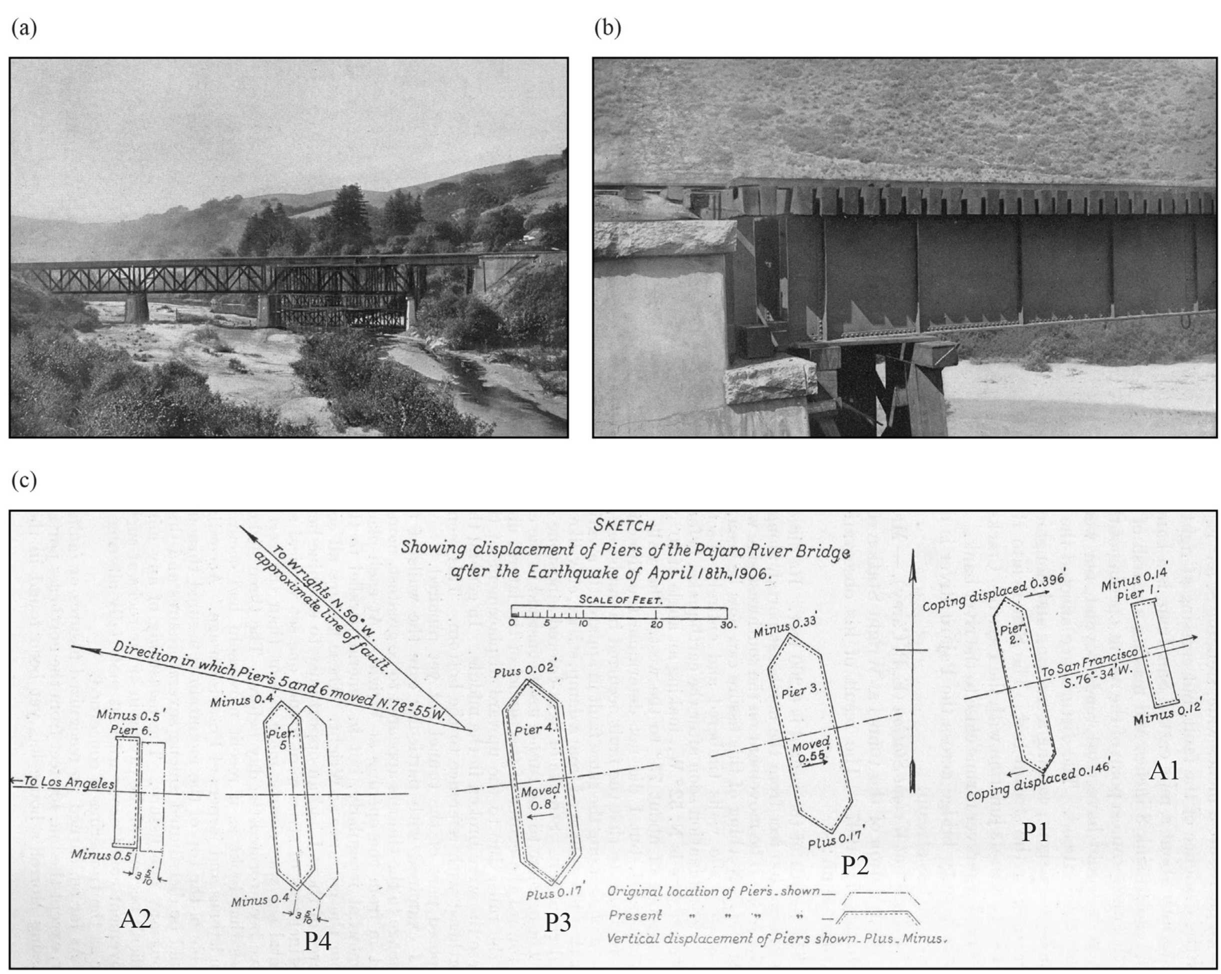

Fig. 3. Pajaro River Bridge during the 1906 San Francisco earthquake: (a) dislocated bridge; (b) displacement at abutment A2; (c) pier displacements (Fig. 3a and b is reprinted from Lawson et al. [70]; Fig. 3c is modified from Lawson et al. [70]).

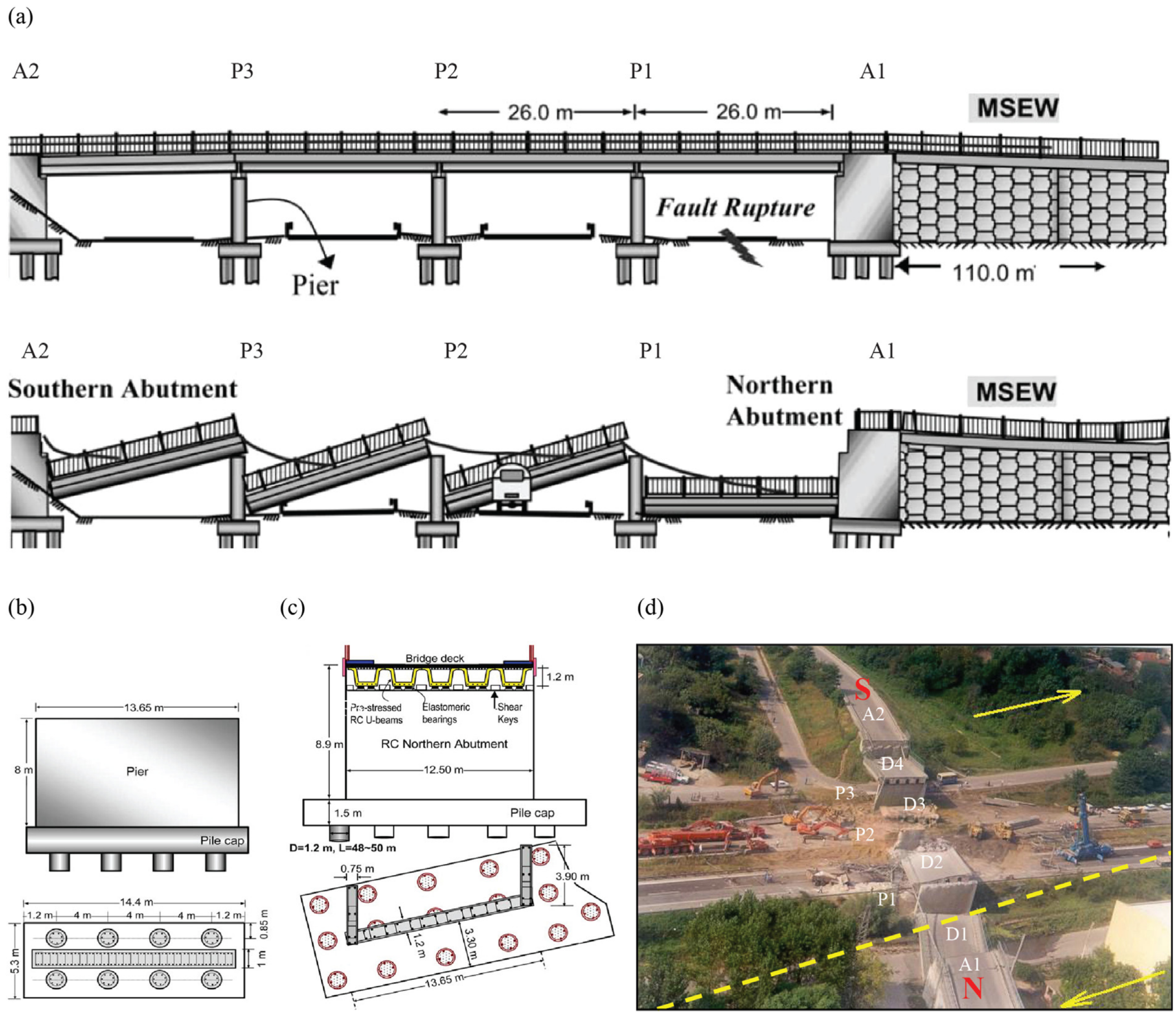

Fig. 4. Arifiye Overpass during the 1999 Kocaeli earthquake: (a) elevation view of bridge before and after the earthquake; (b) detailing of pier and pile foundation; (c) detailing of northeast abutment, deck, and girders; (d) collapsed bridge (Fig. 4a is modified from Pamuk et al. [97]; Fig. 4b and c is reprinted from Pamuk et al. [97]; Fig. 4d is modified from Aydan [7]).

located about 400 m east of the Arifiye Overpass, was a 4-span, simply-supported bridge on wall-type piers. The fault rupture zone crossed the bridge near its northeast abutment (Fig. 5a) resulting in collision between the deck and the abutment and damage to the parapet wall (e.g., [61,62,26,53]). In addition, an approximately 25-mm shear deformation was developed in the transverse direction of the elastomeric bearings. The No. 4 Overpass, located about 400 m west of the Arifiye Overpass, was a 4-span, simply-supported bridge on wall-type piers. The surface fault rupture crossed the bridge at its southwest abutment (Fig. 5a) causing minor damage (e.g., [61,62,26,53]).

The Sakarya Center Bridge (No. 5 Bridge), spanning the Sakarya River near the Trans-European Motorway (Fig. 5a), was a 92-m-long, 8-span (10 m + 6 × 12 m + 10 m), simply-supported steel bridge on steel piles (Fig. 5c). The bridge completely collapsed (Fig. 5d) during the 1999 Kocaeli earthquake primarily due to the fault rupture passing beneath the northwest abutment (e.g., [61,62,26]).

2.3. The 1999 M_w 7.6 Chi-Chi, Taiwan, earthquake

The Pi-Feng Bridge, located downstream of the Shih-Kang Dam on the Ta-Chia River, was an approximately 325-m-long, 13-span, simply-supported, prestressed concrete I-girder bridge (Fig. 6a) supported by single-column piers (Fig. 6c) on caisson foundations (e.g., [2,21,128,142,61,62,129]). The bridge axis was oriented almost in the north-south direction [88,139]. During the 1999 Chi-Chi earthquake, the surface fault rupture propagated in the N20°E–N40°E direction and crossed the bridge between abutment A2 (south abutment) and pier P11 (Fig. 6b) [61,62,139]. A waterfall was created upstream of the bridge (Fig. 6d) as a result of reverse faulting, thus verifying the passing of the fault rupture zone through the bridge. Consequently, the three southernmost spans (D11–D13) collapsed, and pier P11 along with its caisson foundation was uprooted and lay down on the riverbed, as illustrated in Fig. 6b (e.g., [2,21,128,142,61,62,129]). Furthermore, abutment A2 and pier P12 moved upward ~3–4 m and laterally ~3.5–4 m, as shown in Fig. 6b and e [61,62].

The Wu-Shi Bridge, located at the milepost of 210 km + 371 m on Provincial Route 3, was an approximately 625-m-long, dual 18-span, simply-supported, prestressed concrete I-girder bridge (Fig. 7a) supported by wall-type (east bridge) and single-column (west bridge) piers on caisson foundations (Fig. 7b) (e.g., [15,21,50,127,142,61,62,129,65]). The only exceptions were piers P3E, P9E, and P15E of the east bridge, which consisted of two smaller piers connected by a pier wall (e.g., [50,142,65]). The bridge axis was oriented in the N20°E direction (e.g., [61,62,88]). As shown in Fig. 7c, the surface fault rupture of the 1999 Chi-Chi earthquake propagated in the N60°E direction and crossed the bridge between piers P2 and P3 at

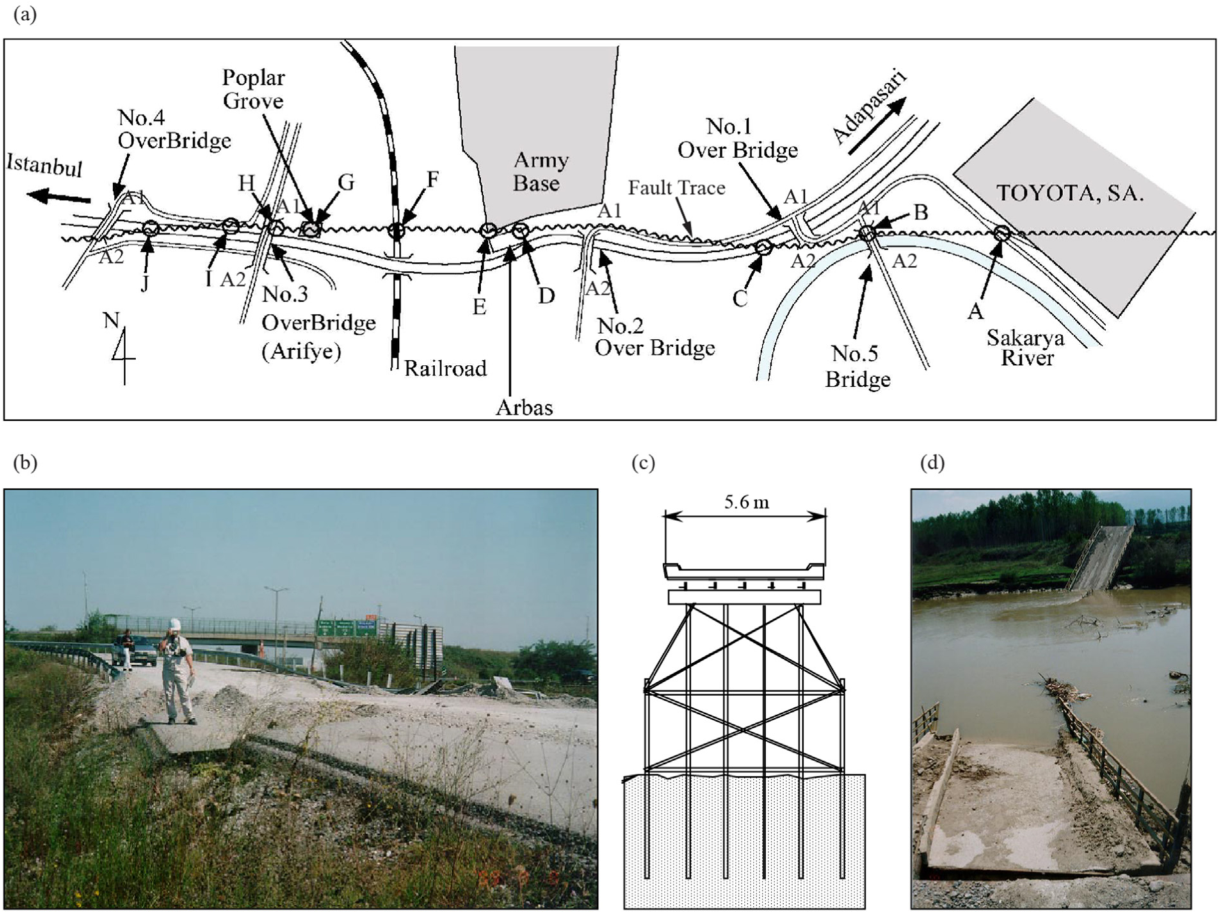

Fig. 5. (a) Surface fault rupture of the 1999 Kocaeli earthquake passing through five bridges; (b) minor damage of No. 1 Overpass; (c) typical section of Sakarya Center Bridge; (d) collapsed Sakarya Center Bridge (Fig. 5a is modified from Kawashima [61,62]; Fig. 5b–d is reprinted from Kawashima [61,62]).

an angle of 40° with respect to its axis [61,62]. After a detailed topographic survey, Kelson et al. [65] reported that the surface fault rupture intersected piers P3W and P3E, where it splayed into a complex series of smaller scarps that bended around individual piers. On the east side of the Wu-Shi Bridge, the individual fault strands rejoined into a single strand that continued northward away from the river valley (Fig. 7c). Though the east and west bridges experienced similar ground motions, they failed in different ways. For the east bridge, spans D1E and D2E collapsed (Fig. 7d) and span D3E exhibited a permanent westward offset (e.g., [2,21,50,65]). However, no shear failures occurred in the piers due to the higher shear capacity of the pier walls; it was only flexural cracks with fractured reinforcement that were observed for pier P3E directly crossed by the fault rupture zone [21]. For the west bridge, nearly all piers suffered damage, but no span collapsed. As shown in Fig. 7e, piers P1W and P2W experienced the most severe shear failure without collapsing (e.g., [127,12,65]).

The Shi-Wei Bridge, located at the milepost of 163 km + 278 m on Provincial Route 3, was an approximately 75-m-long, dual 3-span, skewed and curved, simply-supported, prestressed concrete I-girder bridge (Fig. 8a) supported by single-column piers on caisson foundations (Fig. 8b) (e.g., [2,15,21,142,69,129]). The surface fault rupture of the 1999 Chi-Chi earthquake crossed the bridge in the vicinity of abutment A2 (southeast abutment), imposing significant deformation on the bridge (e.g., [21,129,144]). A 1.5–2 m scarp was visible on the hill above abutment A2, and a retaining wall adjacent to the abutment collapsed toward the river [129]. Two spans of the west bridge (D2W and D3W) and one span of the east bridge (D3E) fell off the piers, as shown in Fig. 8c [15,21,69,144]. Furthermore, piers P1W, P2W, P1E, and P2E tilted considerably, whereas pier P1E suffered shear and flexural cracking in the east-west direction at a height of about 2 m from the ground [69]. Finally, almost all shear keys and elastomeric bearings were damaged during the earthquake.

The E-Jian Bridge, located at the milepost of 25 km + 195 m on County Route 129, was a 264-m-long, 24-span, simply-supported, reinforced concrete double-T-girder bridge (Fig. 9a) supported by wall-type piers on spread footing foundations (Fig. 9b) (e.g., [2,15,21,128,142,129]). The bridge axis was oriented almost in the N50°W direction [88,139]. All spans were supported directly on the piers, without bearings, restrainers and shear keys. During the 1999 Chi-Chi earthquake, the surface fault rupture crossed the bridge between piers P1 and P2 at an angle of 50° with respect to its axis [139]. In addition, as shown in Fig. 9c, surface fault rupture was also observed near abutment A2 (e.g., [128,129,66]). From abutment A1 to pier P12, some piers near the abutment were crushed or snapped, whereas the remaining piers moved toward abutment A2 as rigid bodies or rotated along with their spread footing foundations due to ground movement [21]. As a result, the first nine spans (D1–D9) from abutment A1 collapsed due to displaced or broken piers (Fig. 9d), whereas the remaining spans remained standing with no major damage [15,128,142,34].

The Ming-Tsu Bridge, located at the milepost of 233 km + 564 m on Provincial Route 3, was a 700-m-long, dual 28-span, simply-supported, prestressed concrete I-girder bridge (Fig. 10a) supported by single-column piers on caisson foundations (Fig. 10b) (e.g., [2,15,21,142,129]). During the 1999 Chi-Chi earthquake, surface fault rupture occurred near abutment A2 (southeast abutment), as shown in Fig. 10c (e.g., [15,21,129]). Three spans (D23E, D25E, and D27E) of the east bridge and six spans (D22-25W, D27W, and D28W) of the west

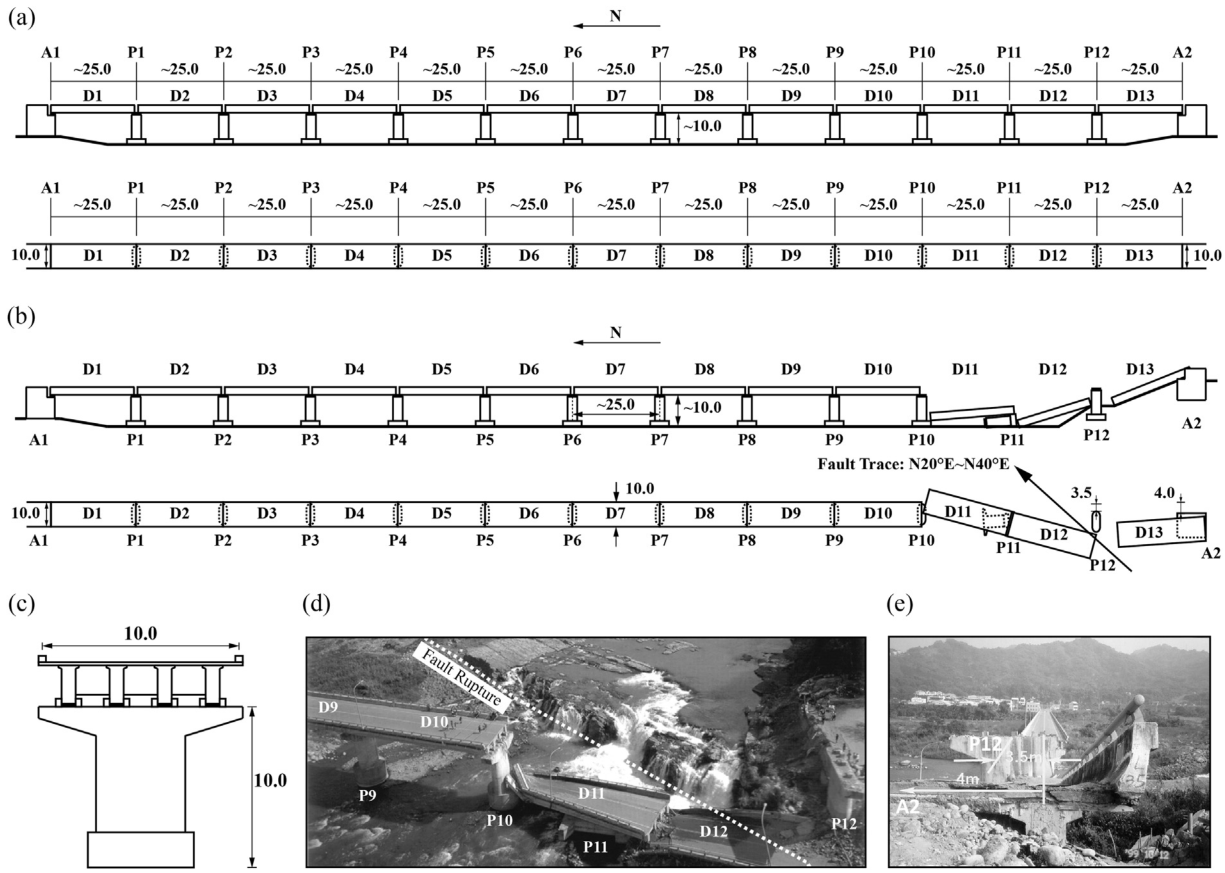

Fig. 6. Pi-Feng Bridge during the 1999 Chi-Chi earthquake: (a) elevation and plan views of original bridge (unit: m); (b) elevation and plan views of collapsed bridge (unit: m); (c) typical section of bridge (unit: m); (d) collapsed bridge and created waterfall; (e) lateral movement of abutment A2 and pier P12 (Fig. 6b is generated based on information provided by Kawashima [61,62]; Fig. 6d is modified from Anastasopoulos et al. [5]; Fig. 6e is modified from Kawashima [61,62]).

bridge collapsed, with a truck and a motorcycle falling off the bridge [142,139]. In addition, the six southernmost piers (P22–P27) sustained significant damage such as cracks, tilting and collapse, whereas the backwall of abutment A2 was impacted by the superstructure and was driven back into the backfill (Fig. 10d) due to the strong longitudinal ground shaking [15,21,142].

The Tong-Tou Bridge, located at the milepost of 13 km + 633 m on County Route 149, was a 160-m-long, 4-span, simply-supported, prestressed concrete I-girder bridge (Fig. 11a) supported by single-column piers on caisson foundations (Fig. 11c). All four spans collapsed and all three piers failed in shear (Fig. 11b and e), as a result of strong ground shaking and fault crossing (Fig. 11d) [15,21,142,129]. Abutment A1 was significantly damaged with its backwall impacted by the superstructure and driven back into the backfill [21], whereas abutment A2 suffered less serious damage. Additionally, significant settlement of the approach pavement was observed just behind abutment A1 [15,21].

The Chang-Geng Bridge, located upstream of the Shih-Kang Dam on the Ta-Chia River, was an approximately 408-m-long, 13-span, simply-supported, prestressed concrete I-girder bridge (Fig. 12a) supported by single-column piers on caisson foundations (Fig. 12c) (e.g., [142,129,119]). During the 1999 Chi-Chi earthquake, spans D11 and D12 near abutment A2 (southwest abutment) collapsed without noticeable damage to the piers, as shown in Fig. 12b and e (e.g., [2,142,128,119]). The observed damage has been attributed primarily to tectonic compression across the bridge caused by two poorly expressed opposite-dipping reverse faults that ruptured near each abutment, as shown in Fig. 12d [12].

The Bauweishan Bridge (Main Line), located on Freeway Route 3 near the Nantou rest area, was a 5-span, slightly curved bridge supported on pile foundations (see figure 3 of [22]). When the 1999 Chi-Chi earthquake occurred, most of the piles of the Bauweishan Bridge had been installed (with some of them completed to the stages of pile cap, pier or cap beam), but the superstructure had not yet been built. At the same site, Ramp 1 was also under construction with only a small number of piles installed, whereas the construction of Ramps 2 and 4 had not yet started. The surface fault rupture crossed the Bauweishan Bridge (Main Line) at pier P1 (see figure 3 of [22]). The piles on the hanging wall were displaced 0.9–2.5 m in the horizontal direction perpendicular to the fault trace, uplifted 1.0–1.6 m, and tilted 1–3°. The piles on the footwall, within a distance of 100 m from the fault trace, were displaced away from the fault, uplifted 0.04–0.08 m, and tilted 1.5–5°. Many of the piles supporting piers were cracked immediately beneath their caps, while piles without piers suffered cracking at deeper locations [22,66]. The Pinlinchi Bridge, located on Freeway Route 3 to the south of Mount Bauweishan, was an 11-span, curved bridge supported on spread footing foundations (piers P1, P2, P8, P9, P10 and abutment A2) and pile foundations (piers P3–P7 and abutment A1). The bridge was under construction when the 1999 Chi-Chi earthquake occurred. The surface fault rupture crossed the Pinlinchi Bridge at pier P10 (see figure 4 of [22]). As a result, the pier was significantly tilted by fault movement and was demolished after the earthquake. The foundations of the remaining piers and of abutment A1 located on the hanging wall were displaced 1.4–2.4 m horizontally and 0.6–1.8 m vertically, whereas the displacement of abutment A2 on the footwall was negligible [22]. The Minchien Viaduct, located on Freeway Route 3 to the south of Mount Choshuishan, consisted of two bridges supported on pile foundations. The bridges were under construction when the 1999 Chi-Chi earthquake occurred. The surface fault rupture crossed the Minchien Viaduct at abutment A1 (see photo 3 of [22]) causing significant displacements and shearing off the piles beneath the

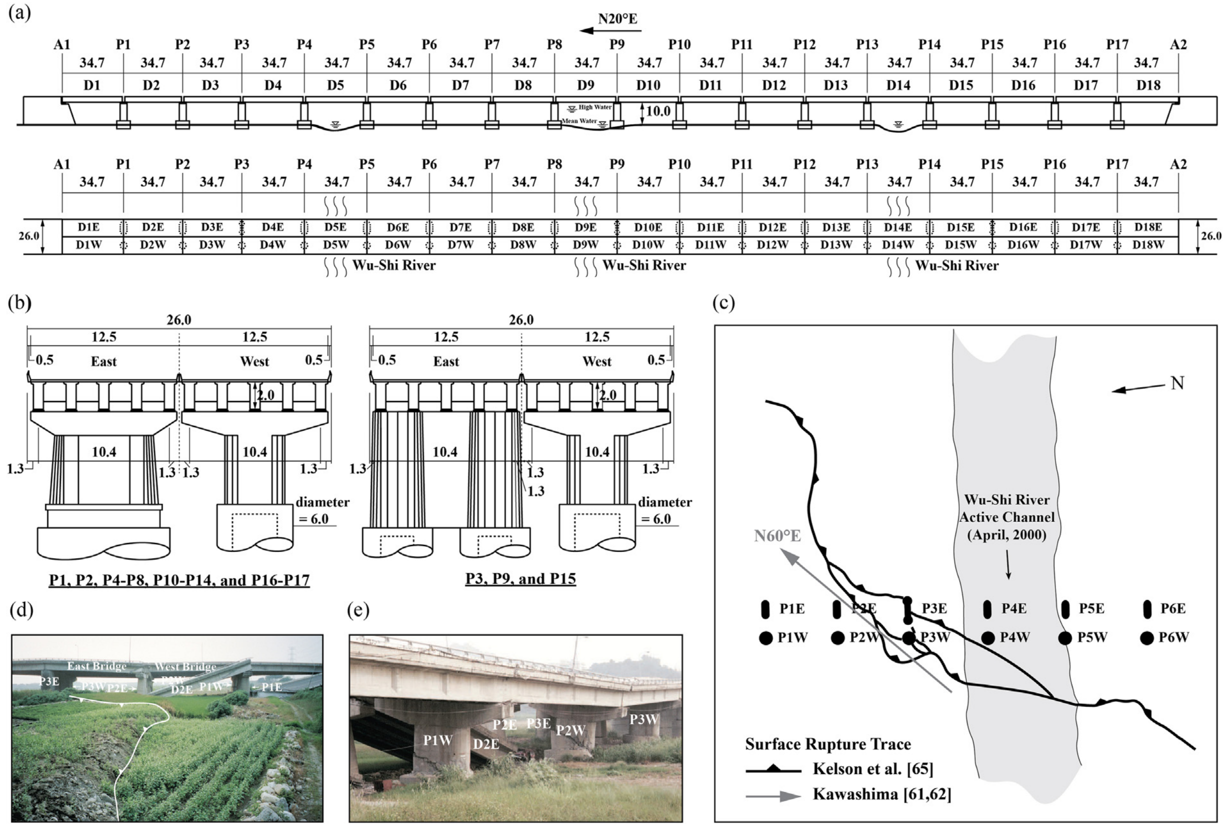

Fig. 7. Wu-Shi Bridge during the 1999 Chi-Chi earthquake: (a) elevation and plan views of original bridge (unit: m); (b) typical sections of bridge (unit: m); (c) map showing bridge crossed by surface fault rupture; (d) collapsed deck; (e) shear failure in piers P1W and P2W (Fig. 7a and b is generated based on information provided by Hsu and Fu [50]; Fig. 7c is generated based on information provided by Kelson et al. [65]; Fig. 7d and e is modified from Kelson et al. [65]).

abutment. Specifically, the horizontal and vertical displacements of the west (respectively, east) segment of abutment A1 were about 1.2 m (respectively, 1.4 m) and 0.8 m (respectively, 0.4 m). On the other hand, the piers sustained small displacements (i.e., maximum horizontal and vertical values were about 0.10 m and 0.08 m, respectively), and were assessed to have no damage after the earthquake [22].

2.4. The 1999 M_w 7.2 Duzce, Turkey, earthquake

Bolu Viaduct 1, a section of the Trans-European Motorway between Bolu and Duzce, was an approximately 2.3-km-long, dual 59-span (with a span length of 39.2 m), simply-supported, seismically isolated, prestressed concrete box-girder bridge supported by varying-height (10–49 m), single-column piers on pile foundations (Fig. 13a) (e.g., [37,56,78,61,62,31,58,100,26,101,98,89,45]). The seismic isolation system consisted of sliding pot bearings along with steel yielding devices (Fig. 13b). The construction of the bridge was almost complete when the 1999 Duzce earthquake occurred. Fig. 13a and d shows that the surface fault rupture crossed the south (eastbound) and north (westbound) bridges between piers P44 and P45 and piers P46 and P47, respectively, at an angle of approximately 20–30° with respect to the longitudinal axis of the bridge (e.g., [61,62,126]). Pier P45 of the south bridge and pier P47 of the north bridge experienced a rigid body rotation of approximately 12° in a clockwise sense (e.g., [26]). In addition, the superstructure sustained a permanent displacement relative to the piers (Fig. 13c), leaving the ends of the girders offset from their supports (e.g., [101]). Furthermore, the sliding bearings and the isolation system were severely damaged (e.g., [37,78,61,62,100,26,89]). The collapse of the superstructure was avoided due to the restraint provided by the shear keys in the transverse direction and the concrete stoppers/cable restrainers in the longitudinal direction [61,62,26,101,5,30].

2.5. The 2008 M_w 7.9 Wenchuan, China, earthquake

The Gaoshu (Yingxiushunhe) Bridge – located in the town of Yingxiu and oriented parallel to the Minjiang River – was an approximately 248-m-long, 18-span, simply-supported, reinforced concrete hollow-slab bridge supported by single-column (A1, P1–P5, P16, P17, and A2) and double-column (P6–P15) piers on pile foundations (Fig. 14a) (e.g., [152,82,53]). With the exception of its deck that was under construction, the bridge was almost complete when the 2008 Wenchuan earthquake occurred. As shown in Fig. 14a and b, the surface fault rupture crossed the bridge between piers P8 and P9 at a nearly right angle [130,132,145,53]. The permanent ground displacements in the horizontal and vertical directions induced by the surface fault rupture were approximately 1 m and 0.5 m near the bridge. These significant residual displacements resulted in the collapse of span D1 followed by the collapse of the remaining spans, as shown in Fig. 14c [130,53]. In addition, flexural-shear failure was observed at the top of several piers [130].

The Xiaoyudong Bridge – crossing the Baishui River in the town of Xiaoyudong – was a 189-m-long, 4-span, simply-supported, reinforced concrete, rigid-frame arch bridge supported by double-column piers on pile foundations (Fig. 15a) (e.g., [8,150,63,151,68,146]). The surface fault rupture crossed the east dyke nearly 70 m upstream of the bridge resulting in an approximately 1.5-m vertical offset, whereas the horizontal residual displacement was negligible. Subsequently, the surface fault rupture extended downstream along the east dyke and crossed the approach road at about 10 m and 50 m behind abutment A1, as illustrated in Fig. 15c (e.g., [63,68]). The angle between the bridge axis and the surface fault rupture was approximately 75° [130]. Fig. 15g

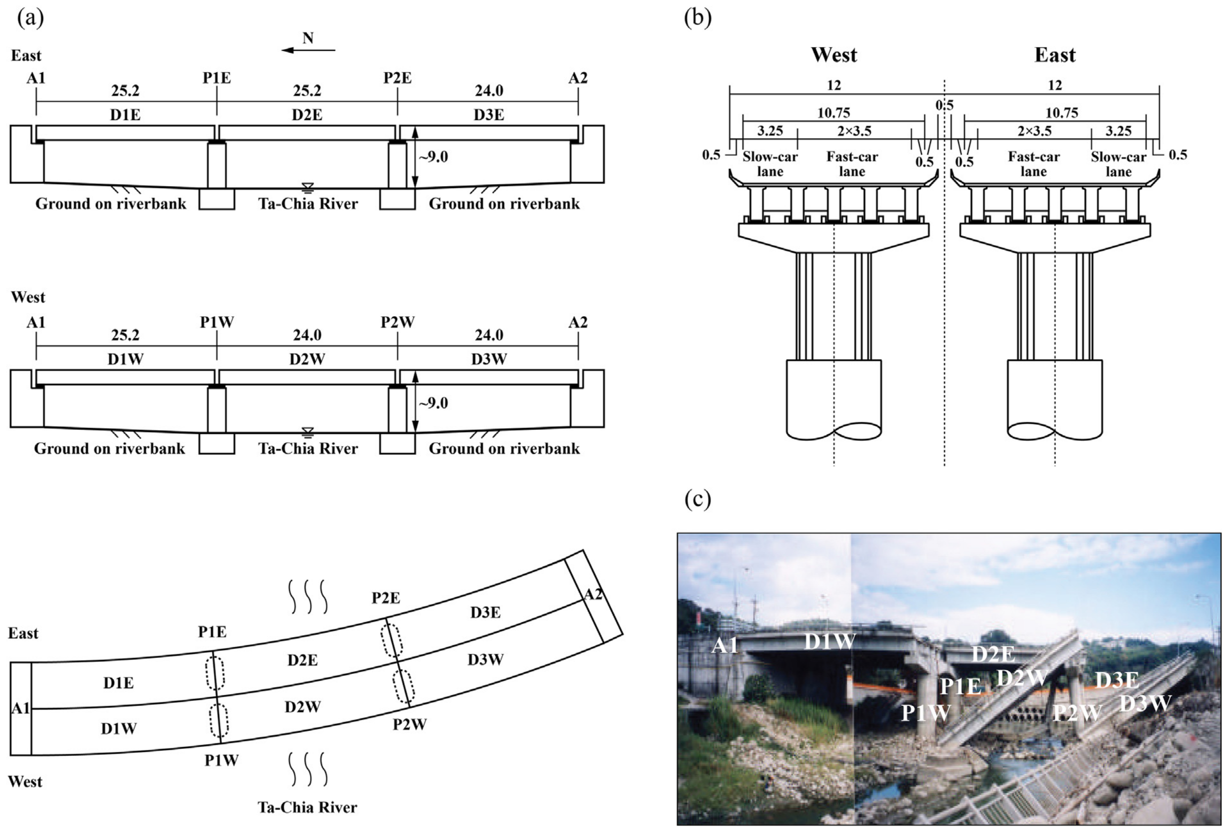

Fig. 8. Shi-Wei Bridge during the 1999 Chi-Chi earthquake: (a) elevation and plan views of original bridge (unit, m); (b) typical section of bridge (unit: m); (c) collapsed bridge (Fig. 8a and b is generated based on information provided by Kosa et al. [69]; Fig. 8c is modified from Kosa et al. [69]).

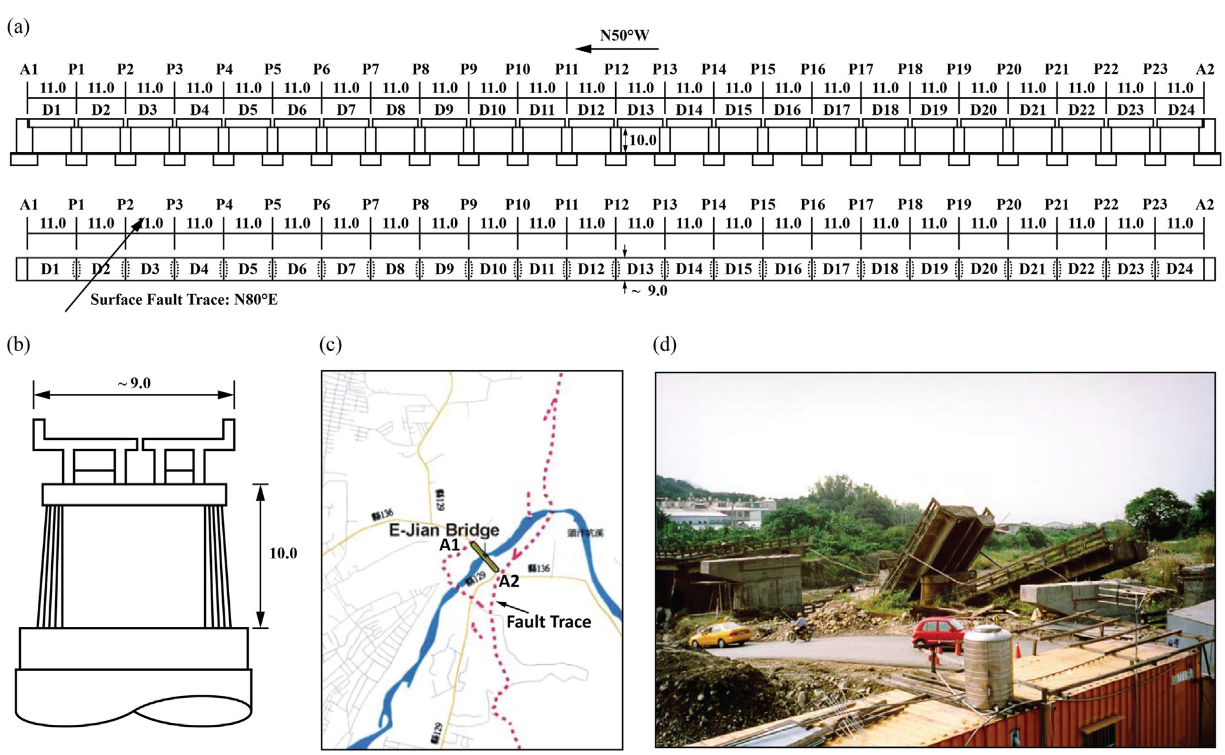

Fig. 9. E-Jian Bridge during the 1999 Chi-Chi earthquake: (a) elevation and plan views of original bridge (unit: m); (b) typical section of bridge (unit: m); (c) map showing bridge crossed by surface fault rupture; (d) collapsed bridge (Fig. 9c is modified from Buckle and Chang [15]; Fig. 9d is reprinted from Buckle and Chang [15]).

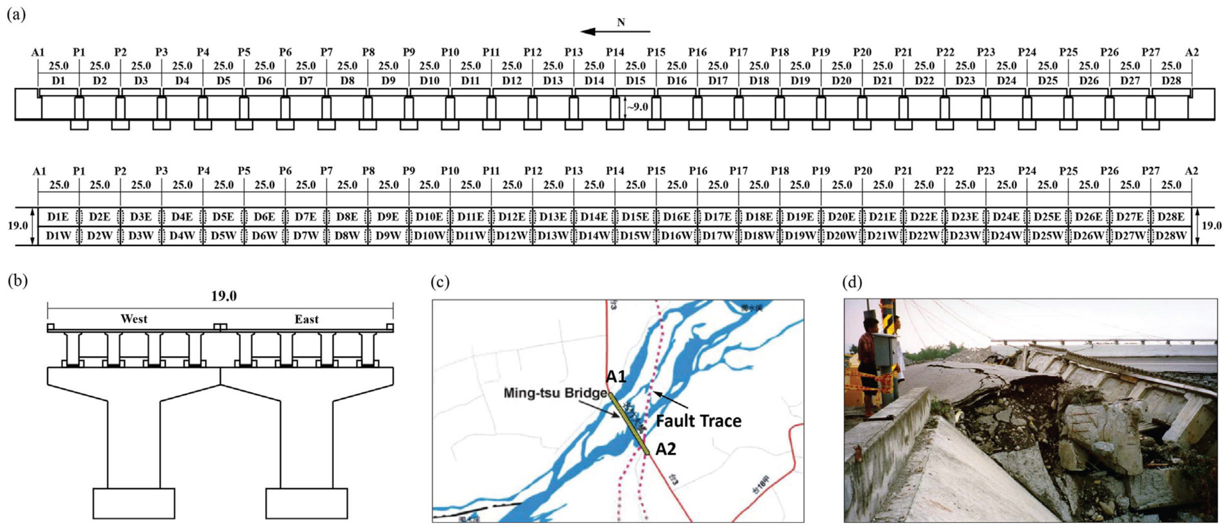

Fig. 10. Ming-Tsu Bridge during the 1999 Chi-Chi earthquake: (a) elevation and plan views of original bridge (unit: m); (b) typical section of bridge (unit: m); (c) map showing bridge crossed by surface fault rupture; (d) failure of backwall and backfill behind southeast abutment (Fig. 10c is modified from Buckle and Chang [15]; Fig. 10d is reprinted from Buckle and Chang [15]).

shows that the approach road behind abutment A1 was severely damaged due to surface fault rupture (e.g., [63,72,116]). As shown in Fig. 15b and e, the two westernmost spans (D3 and D4) collapsed entirely and pier P3 tilted toward abutment A2 [150,63,130,68,146]. In addition, both abutments and span D1 were significantly damaged, as shown in Fig. 15d and f, whereas span D2 suffered less serious damage.

3. Bridges crossing potentially active fault rupture zones

Distinguishing active from inactive faults is an important problem in neotectonics because of the seismic hazard associated with fault activity. The term "active fault" was first introduced by Willis [134], and since then various definitions have been proposed depending on the adopted criteria (e.g., [112,24]). Although none of these definitions is universally accepted, most of them incorporate the following elements: (1) the potential of future fault displacement in the present tectonic setting; and (2) the time of most recent fault displacement (e.g., historical, Holocene or Quaternary) [111]. With regard to fault rupture, the California Department of Transportation (Caltrans) defines as active those faults showing evidence of activation in the last 15,000 years (Holocene or latest Pleistocene) [19,20].

A large number of bridges have been built across potentially active fault rupture zones around the world. These bridges are likely to sustain damage, if not properly designed or retrofitted, due to differential ground displacements across the fault in future large earthquakes. In general, the most common reasons for building a bridge across a fault

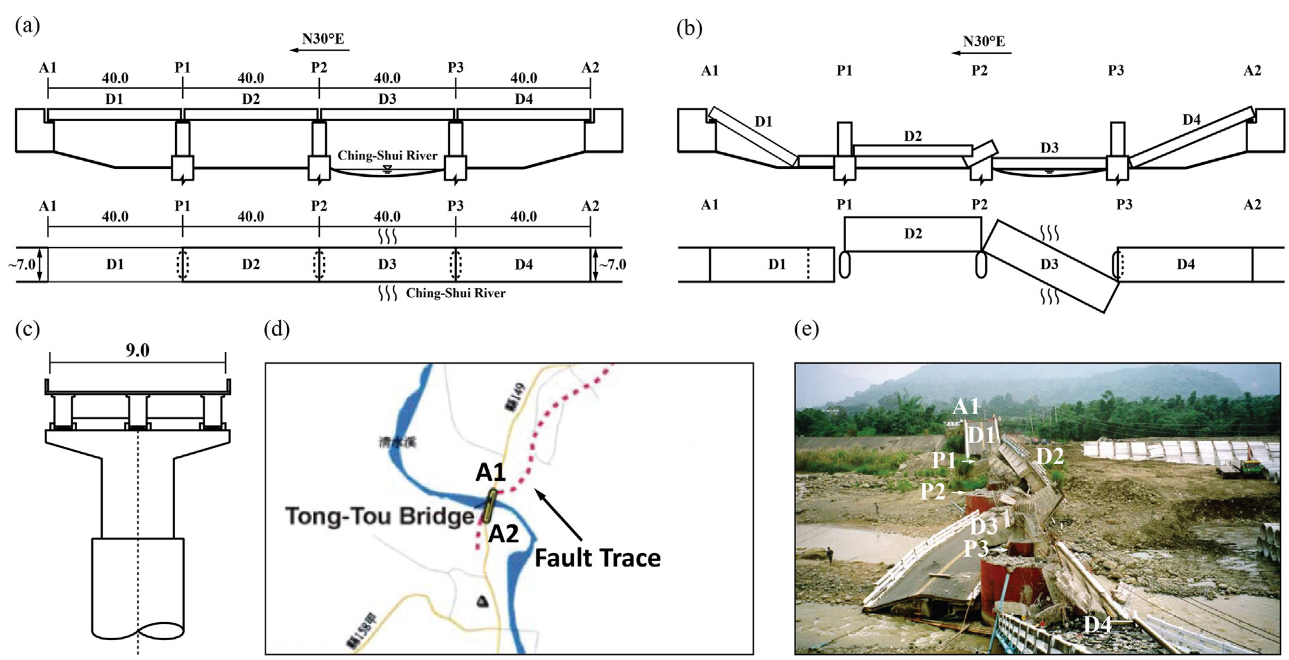

Fig. 11. Tong-Tou Bridge during the 1999 Chi-Chi earthquake: (a) elevation and plan views of original bridge (unit: m); (b) elevation and plan views of collapsed bridge; (c) typical section of bridge (unit: m); (d) map showing bridge crossed by surface fault rupture; (e) collapsed bridge (Fig. 11d and e is modified from Buckle and Chang [15]).

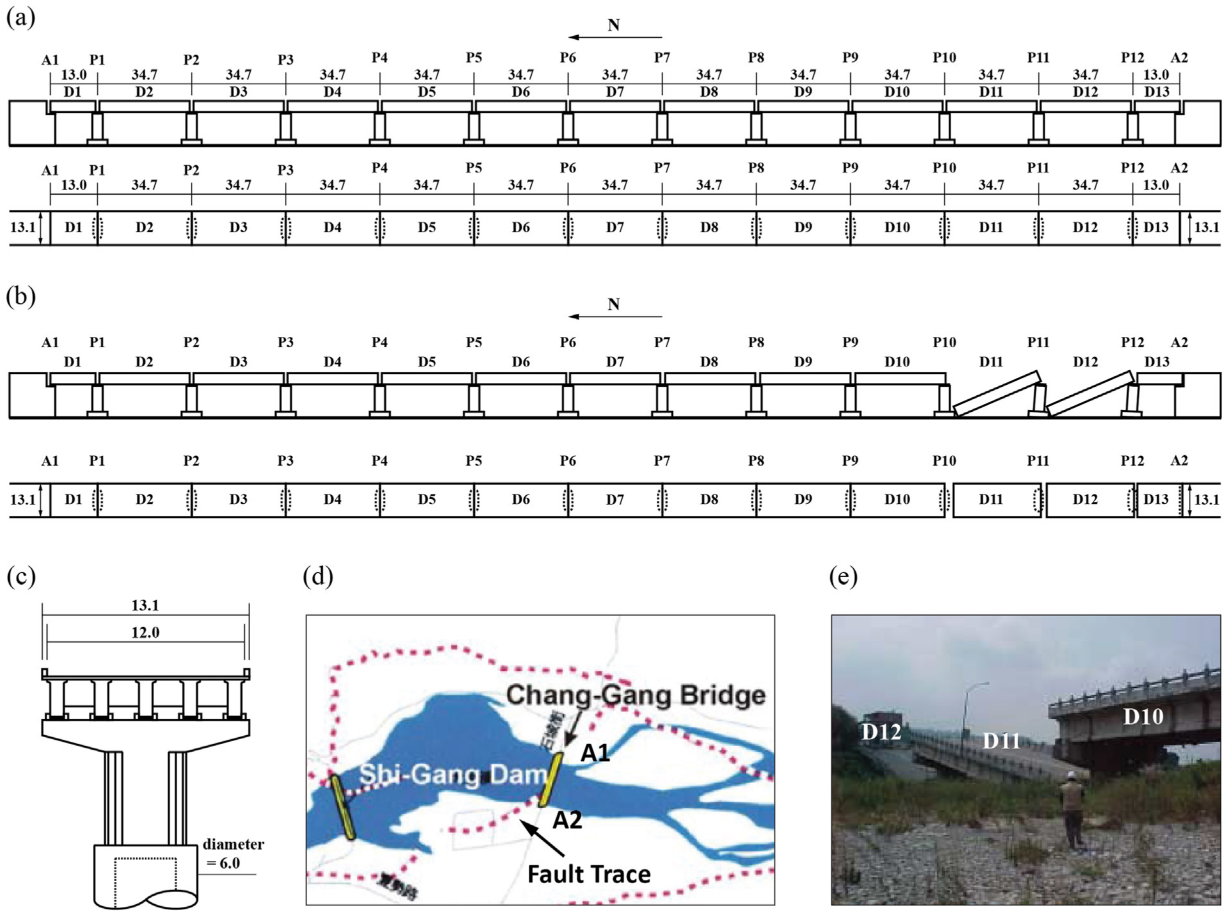

Fig. 12. Chang-Geng Bridge during the 1999 Chi-Chi earthquake: (a) elevation and plan views of original bridge (unit: m); (b) elevation and plan views of collapsed bridge; (c) typical section of bridge (unit: m); (d) map showing bridge crossed by surface fault rupture; (e) two collapsed spans near southwest abutment (Fig. 12a and b is generated based on information provided by Tasaki et al. [119]; Fig. 12d is modified from Buckle and Chang [15]; Fig. 12e is modified from Bray [12]).

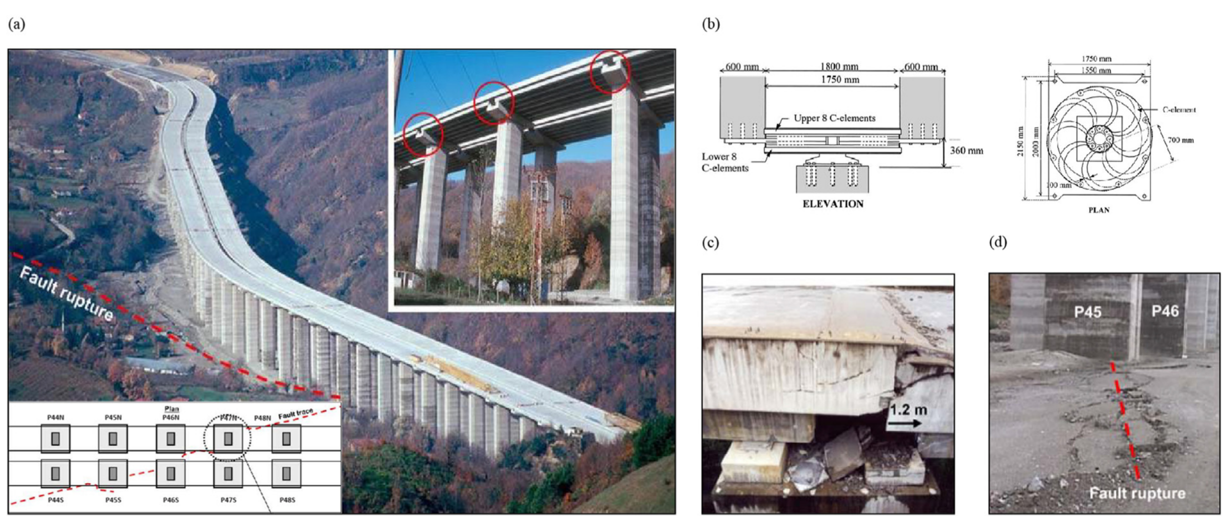

Fig. 13. Bolu Viaduct during the 1999 Duzce earthquake: (a) fault rupture crossing bridge (inset at lower left illustrates fault crossing location); (b) detailing of steel yielding device; (c) displaced superstructure; (d) fault rupture beneath pier P45 (Fig. 13a is modified from Faccioli et al. [30]; Fig. 13c and d is reprinted from Faccioli et al. [30]; Fig. 13b is reprinted from Roussis et al. [101]).

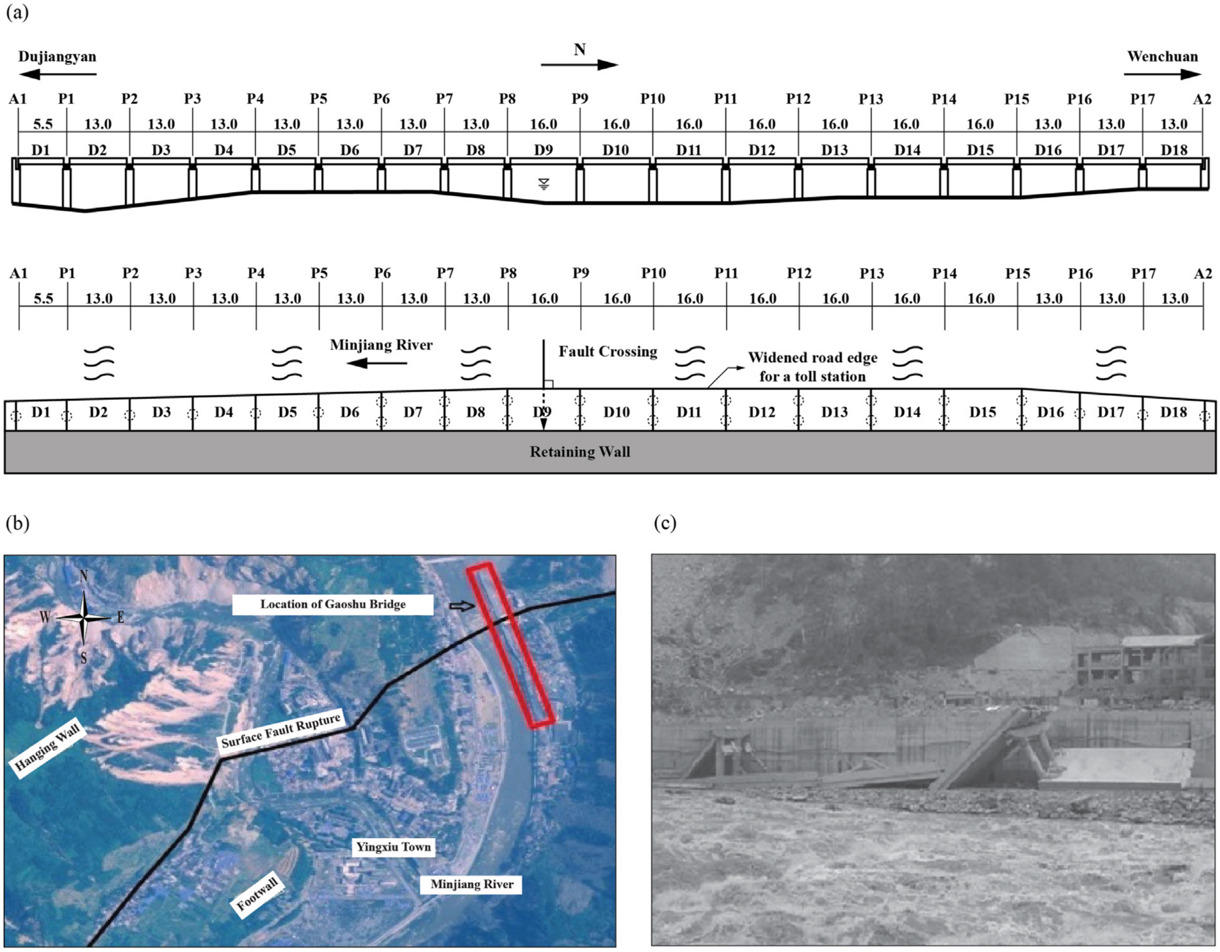

Fig. 14. Gaoshu Bridge during the 2008 Wenchuan earthquake: (a) elevation and plan views of original bridge (unit: m); (b) map showing bridge crossed by surface fault rupture; (c) collapsed bridge (Fig. 14a is generated based on information provided by Hui [53]; Fig. 14b is modified from Hui [53]; Fig. 14c is reprinted from Zhao and Taucer [149]).

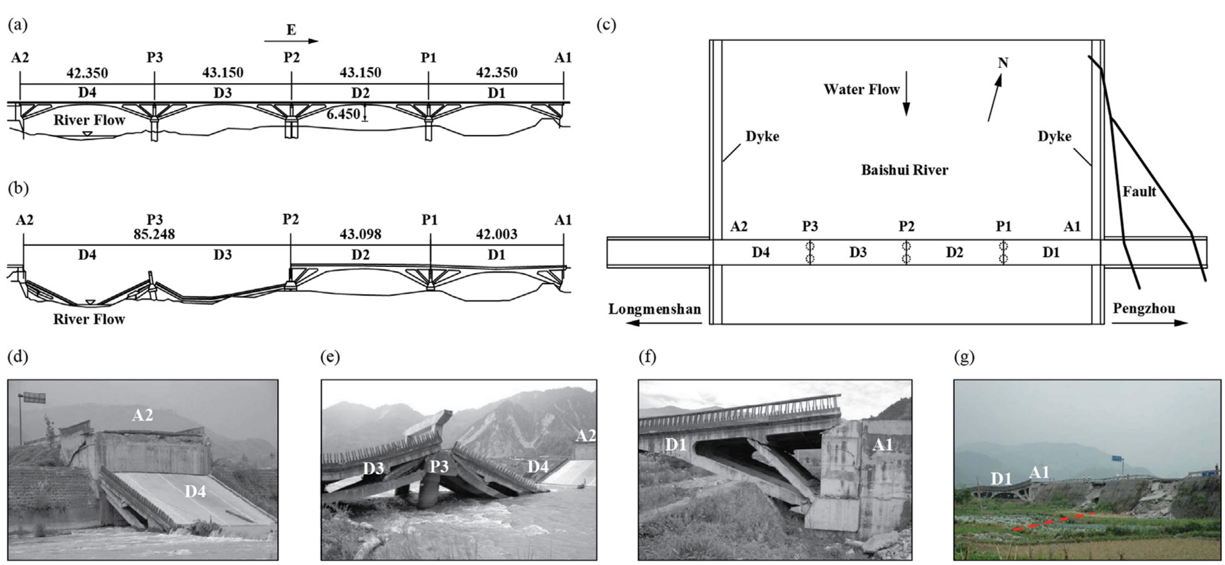

Fig. 15. Xiaoyudong Bridge during the 2008 Wenchuan earthquake: (a) elevation view of original bridge (unit: m); (b) elevation view of collapsed bridge (unit: m); (c) plan view of bridge and surface fault rupture; (d) damaged abutment A2; (e) tilted pier P3 and collapsed spans D3 and D4; (f) damaged span D1 and abutment A1; (g) damaged approach road behind abutment A1 (Fig. 15a–c is generated based on information provided by Kosa et al. [68]; Fig. 15d–f is modified from Kawashima et al. [63]; Fig. 15g is modified from Lin et al. [72]).

Table 2
Bridges crossing potentially active fault rupture zones.

No.	Bridge name or number[a]	Location	Year of completion[b]	Total length (m)[c]	Number of spans[c]	Inter-span relationship[d]	Girder	Pier[e]	Foundation[f]	Bearing[g]	Fault name	Fault type[h]	Reference
1	Puqian Approach Bridge	China	(2019)	581	10	SS & C	Steel box-girder	SCP	PF	N/A	Puqian-Qinglan	NM	[51,110]
2	Mercureaux Viaduct	France	N/A	260	6	N/A	N/A	N/A	PF	N/A	Besancon	RV & SS	[80]
3	Corinth Canal Railway Bridge	Greece	2005	230	3	C	Prestressed concrete box-girder	N/A	SF & PF	LRB	N/A	NM	[77,115]
4	Domokos Railway Bridge	Greece	N/A	422	3	N/A	Steel arch	SCP	CF	SB	Sofades	NM	[5]
5	Thorndon Overbridge	New Zealand	1972/1998	1350	36	SS	Prestressed concrete I-girder	SCP	PF	N/A	Wellington	SS	[11,55,136]
6	San Diego-Coronado Bay Bridge	USA	1969/2002	2381	32	C	Steel box-girder & steel plate girder	DCP	PF & SFF	N/A	Rose Canyon	SS	[6,19,25,33,104,114]
7	Vincent Thomas Bridge	USA	1964/2000	766	3	C	Steel truss	T	PF	N/A	Palos Verdes	OB	[9,57,60,104,113]
Caltrans bridges with a deterministic or probabilistic potential fault offset of more than ~ 0.12 m (0.4 ft)													[19,33,114]
8	Bridge 04-0121	USA	1962/1982	124	4	C	Concrete box-girder	N/A	N/A	N/A	Little Salmon	RV	
9	Bridge 04-0173	USA	1964	57	4	C	Concrete T-girder	N/A	N/A	N/A	Fickle Hill (Mad River)	RV	
10	Bridge 04-0242	USA	1976	83	2	C	Prestressed concrete box-girder	N/A	N/A	N/A	Fickle Hill (Mad River)	RV	
11	Bridge 07-0056	USA	1946	12	3	C	Concrete culvert	N/A	N/A	N/A	Honey Lake	SS	
12	Bridge 10-0001	USA	1957	48	3	N/A	Steel girder	N/A	N/A	N/A	Maacama	SS	
13	Bridge 10-0014	USA	1926/1973	26	3	N/A	Concrete T-girder	N/A	N/A	N/A	Maacama	SS	
14	Bridge 10-0105L	USA	1962	33	3	C	Concrete T-girder	N/A	N/A	N/A	Maacama	SS	
15	Bridge 10-0105R	USA	1962	33	3	C	Concrete T-girder	N/A	N/A	N/A	Maacama	SS	
16	Bridge 10-0116	USA	1947	38	2	C	Steel girder	N/A	N/A	N/A	San Andreas	SS	
17	Bridge 10-0125	USA	1969	32	1	N/A	Prestressed concrete girder	N/A	N/A	N/A	Maacama	SS	
18	Bridge 10-0203L	USA	1962	40	4	C	Concrete T-girder	N/A	N/A	N/A	Maacama	SS	
19	Bridge 10-0203R	USA	1962	40	4	C	Concrete T-girder	N/A	N/A	N/A	Maacama	SS	
20	Bridge 13-0009	USA	1982	52	2	C	Prestressed concrete box-girder	N/A	N/A	N/A	Polaris	SS	
21	Bridge 17-0078	USA	1961/1991	40	3	C	Concrete T-girder	N/A	N/A	N/A	Polaris	SS	
22	Bridge 23-0025	USA	N/A	N/A	N/A	N/A	N/A	N/A	N/A	N/A	Green Valley	SS	
23	Bridge 27-0020	USA	1928	17	3	C	Concrete slab	N/A	N/A	N/A	San Andreas	SS	
24	Bridge 27-0021	USA	1928	17	3	C	Concrete slab	N/A	N/A	N/A	San Andreas	SS	
25	Bridge 27-0122	USA	N/A	N/A	N/A	N/A	N/A	N/A	N/A	N/A	San Andreas	SS	
26	Bridge 28-0186	USA	1963/2000	113	4	C	Concrete box-girder	N/A	N/A	N/A	Concord	SS	
27	Bridge 28-0186K	USA	1996	49	1	N/A	Prestressed concrete box-girder	N/A	N/A	N/A	Concord	SS	
28	Bridge 28-0240L	USA	1981	130	5	C	Concrete box-girder	N/A	N/A	N/A	Concord	SS	
29	Bridge 28-0240R	USA	1981	128	5	C	Concrete box-girder	N/A	N/A	N/A	Concord	SS	
30	Bridge 33-0026L	USA	1969	91	3	C	Concrete box-girder	N/A	N/A	N/A	Greenville	SS	
31	Bridge 33-0026R	USA	1969	56	3	C	Concrete box-girder	N/A	N/A	N/A	Greenville	SS	
32	Bridge 33-0121L	USA	1969	140	6	C	Concrete box-girder	N/A	N/A	N/A	Greenville	SS	
33	Bridge 33-0121R	USA	1938/1969	140	10	C	Concrete T-girder	N/A	N/A	N/A	Greenville	SS	
34	Bridge 33-0159	USA	1956	41	2	C	Concrete box-girder	N/A	N/A	N/A	Hayward	SS	
35	Bridge 33-0160	USA	1956	33	2	C	Concrete slab	N/A	N/A	N/A	Hayward	SS	
36	Bridge 33-0161	USA	N/A	N/A	N/A	N/A	N/A	N/A	N/A	N/A	Hayward	SS	
37	Bridge 33-0162	USA	1951	36	2	C	Concrete T-girder	N/A	N/A	N/A	Hayward	SS	
38	Bridge 33-0164K	USA	1951	8	1	N/A	Steel arch	N/A	N/A	N/A	Hayward	SS	
39	Bridge 33-0211	USA	1977	114	2	C	Prestressed concrete box-girder	N/A	N/A	N/A	Calaveras	SS	
40	Bridge 33-0244	USA	N/A	N/A	N/A	N/A	N/A	N/A	N/A	N/A	Hayward	SS	

(*continued on next page*)

Table 2 (*continued*)

No.	Bridge name or number[a]	Location	Year of completion[b]	Total length (m)[c]	Number of spans[c]	Inter-span relationship[d]	Girder	Pier[e]	Foundation[f]	Bearing[g]	Fault name	Fault type[h]	Reference
41	Bridge 33-0343	USA	1965	34	3	C	Concrete box-girder	N/A	N/A	N/A	Hayward	SS	
42	Bridge 33-0347S	USA	1965	88	3	C	Concrete box-girder	N/A	N/A	N/A	Hayward	SS	
43	Bridge 33-0351	USA	1963/1990	45	3	C	Concrete box-girder	N/A	N/A	N/A	Calaveras	SS	
44	Bridge 33-0352	USA	1967/1990	101	3	C	Concrete box-girder	N/A	N/A	N/A	Calaveras	SS	
45	Bridge 33-0354	USA	1965	55	3	C	Concrete box-girder	N/A	N/A	N/A	Hayward	SS	
46	Bridge 33-0424L	USA	1971/1997	49	2	C	Concrete box-girder	N/A	N/A	N/A	Hayward	SS	
47	Bridge 33-0424R	USA	1971/1997	51	2	C	Concrete box-girder	N/A	N/A	N/A	Hayward	SS	
48	Bridge 33-0427L	USA	1971/2010	67	2	C	Prestressed concrete box-girder	N/A	N/A	N/A	Hayward	SS	
49	Bridge 33-0427R	USA	1971/1997	78	2	C	Prestressed concrete box-girder	N/A	N/A	N/A	Hayward	SS	
50	Bridge 33-0428R	USA	1971/1997	54	2	C	Concrete box-girder	N/A	N/A	N/A	Hayward	SS	
51	Bridge 33-0438L	USA	1971/2010	70	3	C	Concrete box-girder	N/A	N/A	N/A	Hayward	SS	
52	Bridge 33-0438R	USA	1971/1997	67	3	C	Concrete box-girder	N/A	N/A	N/A	Hayward	SS	
53	Bridge 33-0439L	USA	1971/2010	32	1	N/A	Prestressed concrete box-girder	N/A	N/A	N/A	Hayward	SS	
54	Bridge 33-0439R	USA	1971/1997	32	1	N/A	Prestressed concrete box-girder	N/A	N/A	N/A	Hayward	SS	
55	Bridge 33-0607F	USA	1998	13	1	N/A	Concrete frame	N/A	N/A	N/A	Hayward	SS	
56	Bridge 35-0044	USA	1903	7	1	N/A	Concrete arch	N/A	N/A	N/A	San Andreas	SS	
57	Bridge 35-0192	USA	1964/1972	41	3	C	Concrete box-girder	N/A	N/A	N/A	San Andreas	SS	
58	Bridge 37-0006L	USA	1970	205	6	C	Concrete box-girder	N/A	N/A	N/A	Sargent	SS	
59	Bridge 37-0006R	USA	1950	185	11	N/A	Steel girder	N/A	N/A	N/A	Sargent	SS	
60	Bridge 37-0073	USA	1924/1934	17	1	N/A	Concrete T-girder	N/A	N/A	N/A	San Andreas	SS	
61	Bridge 43-0015	USA	1955	54	3	N/A	Steel girder	N/A	N/A	N/A	San Andreas	SS	
62	Bridge 48-0070L	USA	2000	12	4	C	Concrete culvert	N/A	N/A	N/A	Owens Valley	SS	
63	Bridge 50-0048	USA	1951/1997	40	4	C	Concrete slab	N/A	N/A	N/A	Garlock	SS	
64	Bridge 50-0347	USA	1970	66	2	C	Concrete box-girder	N/A	N/A	N/A	Garlock	SS	
65	Bridge 52-0009	USA	1987	74	4	C	Concrete box-girder	N/A	N/A	N/A	N/A	N/A	
66	Bridge 52-0329	USA	1970	81	2	C	Prestressed concrete box-girder	N/A	N/A	N/A	Simi-Santa Rosa	RV	
67	Bridge 52-0346L	USA	1970	31	1	N/A	Prestressed concrete box-girder	N/A	N/A	N/A	Simi-Santa Rosa	RV	
68	Bridge 52-0346R	USA	1970	31	1	N/A	Prestressed concrete box-girder	N/A	N/A	N/A	Simi-Santa Rosa	RV	
69	Bridge 52-0348	USA	1972	164	5	C	Concrete box-girder	N/A	N/A	N/A	Simi-Santa Rosa	RV	
70	Bridge 53-0030	USA	1947	6	1	N/A	Concrete culvert	N/A	N/A	N/A	N/A	N/A	
71	Bridge 53-0434	USA	1938	27	2	C	Concrete slab	N/A	N/A	N/A	Raymond	SS	
72	Bridge 53-0435	USA	1939	27	2	C	Concrete slab	N/A	N/A	N/A	Raymond	SS	
73	Bridge 53-0436	USA	1939	26	2	C	Concrete slab	N/A	N/A	N/A	Raymond	SS	
74	Bridge 53-0437	USA	1940	26	2	C	Concrete slab	N/A	N/A	N/A	Raymond	SS	
75	Bridge 53-0438	USA	1940	26	2	C	Concrete slab	N/A	N/A	N/A	Raymond	SS	
76	Bridge 53-0439	USA	N/A	N/A	N/A	N/A	N/A	N/A	N/A	N/A	Raymond	SS	
77	Bridge 53-0440	USA	1940	27	2	C	Concrete slab	N/A	N/A	N/A	Raymond	SS	
78	Bridge 53-0679	USA	1952/1977	50	1	N/A	Concrete box-girder	N/A	N/A	N/A	Hollywood	SS	
79	Bridge 53-0680	USA	1953/1977	184	7	C	Concrete box-girder	N/A	N/A	N/A	Hollywood	SS	
80	Bridge 53-0848	USA	1955/1984	72	3	C	Concrete box-girder	N/A	N/A	N/A	Sierra Madre (Santa Susana)	RV	
81	Bridge 53-0853	USA	1954/2003	34	1	N/A	Prestressed concrete box-girder	N/A	N/A	N/A	San Jose	SS	
82	Bridge 53-0854	USA	1954/2003	29	1	N/A	Prestressed concrete box-girder	N/A	N/A	N/A	San Jose	SS	
83	Bridge 53-0855	USA	1954/2003	251	10	N/A	Prestressed concrete box-girder	N/A	N/A	N/A	San Jose	SS	

(*continued on next page*)

Table 2 (*continued*)

No.	Bridge name or number[a]	Location	Year of completion[b]	Total length (m)[c]	Number of spans[c]	Inter-span relationship[d]	Girder	Pier[e]	Foundation[f]	Bearing[g]	Fault name	Fault type[h]	Reference
84	Bridge 53-0865K	USA	1977	89	3	C	Prestressed concrete box-girder	N/A	N/A	N/A	Hollywood	SS	
85	Bridge 53-1011	USA	1955/1970	15	1	N/A	Concrete slab	N/A	N/A	N/A	Sierra Madre (Santa Susana)	RV	
86	Bridge 53-1012	USA	1970	21	1	N/A	Concrete T-girder	N/A	N/A	N/A	Sierra Madre (Santa Susana)	RV	
87	Bridge 53-1097	USA	1959/2013	21	1	N/A	Concrete box-girder	N/A	N/A	N/A	Santa Monica	SS	
88	Bridge 53-1183	USA	N/A	N/A	N/A	N/A	N/A	N/A	N/A	N/A	Hollywood	SS	
89	Bridge 53-1207	USA	1963/1996	62	3	C	Concrete box-girder	N/A	N/A	N/A	Newport-Inglewood	SS	
90	Bridge 53-1208	USA	1963	168	5	C	Concrete box-girder	N/A	N/A	N/A	Newport-Inglewood	SS	
91	Bridge 53-1417	USA	1966/2006	52	4	C	Concrete T-girder	N/A	N/A	N/A	San Andreas	SS	
92	Bridge 53-1776L	USA	1966	30	3	C	Concrete T-girder	N/A	N/A	N/A	Garlock	SS	
93	Bridge 53-1776R	USA	1966	30	3	C	Concrete T-girder	N/A	N/A	N/A	Garlock	SS	
94	Bridge 53-1779	USA	1966	71	2	C	Concrete box-girder	N/A	N/A	N/A	San Andreas	SS	
95	Bridge 53-1986	USA	1971/1973	205	7	C	Concrete box-girder	N/A	N/A	N/A	Sierra Madre (Santa Susana)	RV	
96	Bridge 53-2000G	USA	1972	41	1	N/A	Prestressed concrete box-girder	N/A	N/A	N/A	San Jose (groundwater barrier)	SS	
97	Bridge 53-2001F	USA	1972	42	1	N/A	Prestressed concrete box-girder	N/A	N/A	N/A	San Jose (groundwater barrier)	SS	
98	Bridge 53-2003	USA	1972	198	6	C	Concrete box-girder	N/A	N/A	N/A	San Jose (groundwater barrier)	SS	
99	Bridge 53-2004G	USA	1972	216	6	C	Concrete box-girder	N/A	N/A	N/A	San Jose (groundwater barrier)	SS	
100	Bridge 53-2006G	USA	1972	185	6	C	Concrete box-girder	N/A	N/A	N/A	San Jose (groundwater barrier)	SS	
101	Bridge 53-2007F	USA	1972	273	7	C	Concrete box-girder	N/A	N/A	N/A	San Jose (groundwater barrier)	SS	
102	Bridge 53-2102G	USA	1975	508	5	C	Prestressed concrete box-girder	N/A	N/A	N/A	Sierra Madre (Tujunga)	RV	
103	Bridge 53-2105G	USA	1975	71	3	C	Concrete box-girder	N/A	N/A	N/A	Sierra Madre (Tujunga)	RV	
104	Bridge 53-2113	USA	1975	54	3	C	Concrete box-girder	N/A	N/A	N/A	Sierra Madre (Tujunga)	RV	
105	Bridge 53-2185M	USA	1967	7	2	N/A	Concrete culvert	N/A	N/A	N/A	San Andreas	SS	
106	Bridge 53-2707	USA	N/A	N/A	N/A	N/A	N/A	N/A	N/A	N/A	Newport-Inglewood	SS	
107	Bridge 54-0422	USA	1967	102	6	C	Concrete box-girder	N/A	N/A	N/A	San Jacinto	SS	
108	Bridge 54-0471F	USA	1964/1972	235	12	C	Concrete T-girder	N/A	N/A	N/A	San Jacinto	SS	
109	Bridge 54-0471L	USA	1958/1972	225	12	C	Concrete T-girder	N/A	N/A	N/A	San Jacinto	SS	
110	Bridge 54-0471R	USA	1972	216	12	C	Concrete T-girder	N/A	N/A	N/A	San Jacinto	SS	
111	Bridge 54-0482G	USA	1959	231	6	N/A	Steel girder	N/A	N/A	N/A	San Jacinto	SS	
112	Bridge 54-0482L	USA	1959/1972	228	6	N/A	Steel girder	N/A	N/A	N/A	San Jacinto	SS	
113	Bridge 54-0482R	USA	1973	228	6	N/A	Steel girder	N/A	N/A	N/A	San Jacinto	SS	
114	Bridge 54-0569	USA	1958	10	3	N/A	Concrete culvert	N/A	N/A	N/A	Helendale-South Lockhart	SS	
115	Bridge 54-0632	USA	1963	75	4	C	Concrete box-girder	N/A	N/A	N/A	Calico-Hidalgo (Calico)	SS	
116	Bridge 54-0772L	USA	1969	41	3	C	Concrete box-girder	N/A	N/A	N/A	San Andreas (San Bernardino Mountains)	NM	
117	Bridge 54-0772R	USA	1969/2007	48	3	C	Concrete box-girder	N/A	N/A	N/A	San Andreas (San Bernardino Mountains)	NM	
118	Bridge 54-0821F	USA	1972	32	1	N/A	Prestressed concrete box-girder	N/A	N/A	N/A	San Jacinto	SS	
119	Bridge 54-0822F	USA	1972	800	4	C	Prestressed concrete box-girder	N/A	N/A	N/A	San Jacinto	SS	
120	Bridge 54-0823G	USA	1972	774	8	C	Prestressed concrete box-girder	N/A	N/A	N/A	San Jacinto	SS	
121	Bridge 54-0916	USA	1969	6	1	N/A	Steel culvert	N/A	N/A	N/A	San Andreas	SS	

(*continued on next page*)

Table 2 (*continued*)

No.	Bridge name or number[a]	Location	Year of completion[b]	Total length (m)[c]	Number of spans[c]	Inter-span relationship[d]	Girder	Pier[e]	Foundation[f]	Bearing[g]	Fault name	Fault type[h]	Reference
122	Bridge 54-1043	USA	1976	62	3	C	Concrete T-girder	N/A	N/A	N/A	San Jacinto	SS	
123	Bridge 54-1047	USA	1973	8	2	N/A	Concrete culvert	N/A	N/A	N/A	Helendale-South Lockhart	SS	
124	Bridge 54-1086	USA	1993	44	1	N/A	Prestressed concrete box-girder	N/A	N/A	N/A	San Andreas (San Bernardino South)	SS	
125	Bridge 54-1160L	USA	2007	49	1	N/A	Prestressed concrete box-girder	N/A	N/A	N/A	San Jacinto	SS	
126	Bridge 54-1160R	USA	2007	49	1	N/A	Prestressed concrete box-girder	N/A	N/A	N/A	San Jacinto	SS	
127	Bridge 54-1161	USA	2007	170	4	C	Prestressed concrete box-girder	N/A	N/A	N/A	San Jacinto	SS	
128	Bridge 54-1283	USA	2010	21	1	N/A	Concrete box-girder	N/A	N/A	N/A	Helendale-South Lockhart	SS	
129	Bridge 55-0602K	USA	1971	13	3	N/A	Concrete culvert	N/A	N/A	N/A	Whittier (Elsinore)	SS	
130	Bridge 56-0284	USA	1951/1997	8	3	N/A	Concrete culvert	N/A	N/A	N/A	San Andreas	SS	
131	Bridge 56-0285	USA	1951/1997	16	4	N/A	Concrete culvert	N/A	N/A	N/A	San Andreas	SS	
132	Bridge 56-0454	USA	1964/1970	38	3	C	Concrete box-girder	N/A	N/A	N/A	San Gorgonio	RV	
133	Bridge 56-0492	USA	1952	9	2	N/A	Concrete culvert	N/A	N/A	N/A	San Jacinto	SS	
134	Bridge 56-0637	USA	1970/1992	95	3	C	Concrete box-girder	N/A	N/A	N/A	Elsinore (Chino)	SS	
135	Bridge 57-0166	USA	N/A	N/A	N/A	N/A	N/A	N/A	N/A	N/A	Elsinore	SS	
136	Bridge 57-0287L	USA	1954/1969	52	3	C	Concrete box-girder	N/A	N/A	N/A	Rose Canyon (San Diego)	SS	
137	Bridge 57-0287R	USA	1969	29	1	N/A	Concrete box-girder	N/A	N/A	N/A	Rose Canyon (San Diego)	SS	
138	Bridge 57-0288	USA	1954/1969	57	3	C	Concrete box-girder	N/A	N/A	N/A	Rose Canyon (San Diego)	SS	
139	Bridge 57-0289	USA	1954/1965	136	6	C	Concrete box-girder	N/A	N/A	N/A	Rose Canyon (San Diego)	SS	
140	Bridge 57-0457	USA	1966	186	4	N/A	Steel girder	N/A	N/A	N/A	Rose Canyon (San Diego)	SS	
141	Bridge 57-0463F	USA	1966	109	6	C	Concrete box-girder	N/A	N/A	N/A	Rose Canyon (San Diego)	SS	
142	Bridge 57-0518G	USA	1966	72	3	C	Concrete box-girder	N/A	N/A	N/A	Rose Canyon (San Diego)	SS	
143	Bridge 57-0519F	USA	1966	74	3	C	Concrete box-girder	N/A	N/A	N/A	Rose Canyon (San Diego)	SS	
144	Bridge 57-0520L	USA	1966	537	17	C	Concrete box-girder	N/A	N/A	N/A	Rose Canyon (San Diego)	SS	
145	Bridge 57-0521F	USA	1966	107	4	C	Concrete box-girder	N/A	N/A	N/A	Rose Canyon (San Diego)	SS	
146	Bridge 57-0522F	USA	1966	79	3	C	Concrete box-girder	N/A	N/A	N/A	Rose Canyon (San Diego)	SS	
147	Bridge 57-0523F	USA	1966	80	3	C	Concrete box-girder	N/A	N/A	N/A	Rose Canyon (San Diego)	SS	

Note: N/A = not available.

[a] Bridge numbers can be used to acquire additional information about Caltrans bridges from accessible files provided by FHWA [33] and Caltrans [19]. The San Diego-Coronado Bay Bridge, which is listed as bridge No. 6, is also within the 141 potential fault-crossing bridges identified by Caltrans [19].

[b] Year of completion is provided for all bridges. Expected year of completion is provided in parentheses for Puqian Approach Bridge. Year of retrofit is also provided for Thorndon Overbridge, San Diego-Coronado Bay Bridge, and Vincent Thomas Bridge. Year of most recent reconstruction is also provided for Caltrans bridges if available.

[c] Total length and number of spans are provided for the main bridge of San Diego-Coronado Bay Bridge and Vincent Thomas Bridge.

[d] SS, simply-supported; C, continuous.

[e] SCP, single-column pier; DCP, double-column pier; T, tower.

[f] PF, pile foundation; SF, shaft foundation; SFF, spread footing foundation.

[g] LRB, lead rubber bearing; SB, spherical bearing.

[h] SS, strike-slip; RV, reverse; NM, normal; OB, oblique.

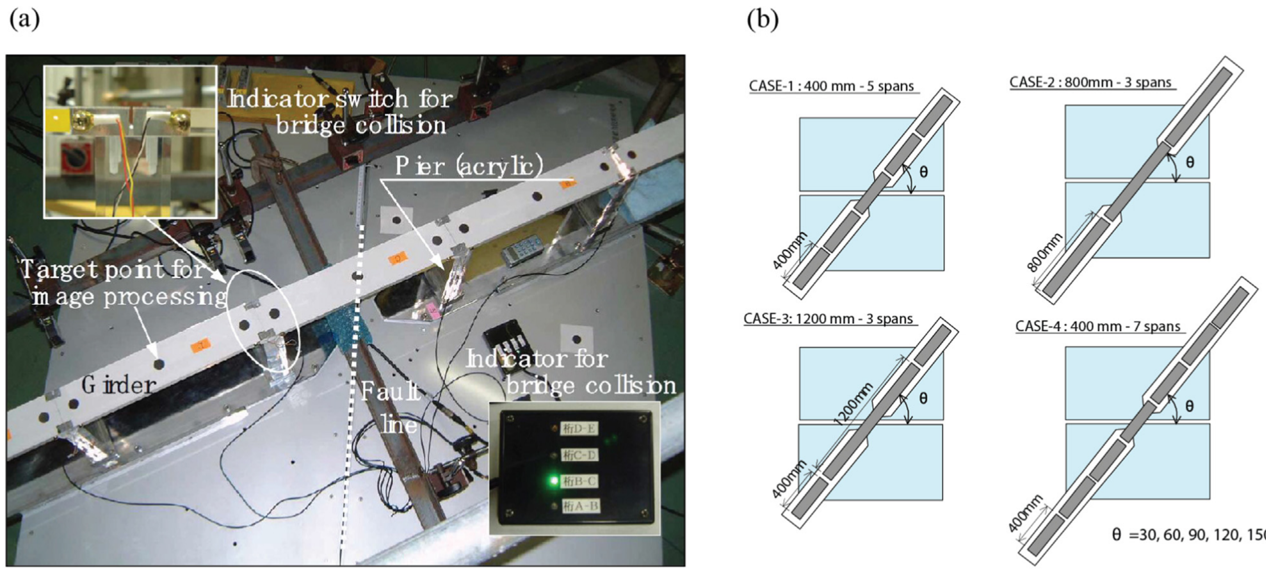

Fig. 16. Experiment of a small-scale (1/50) bridge model subjected to fault rupture: (a) experimental device; (b) test cases (all figures are reprinted from Murono et al. [92]).

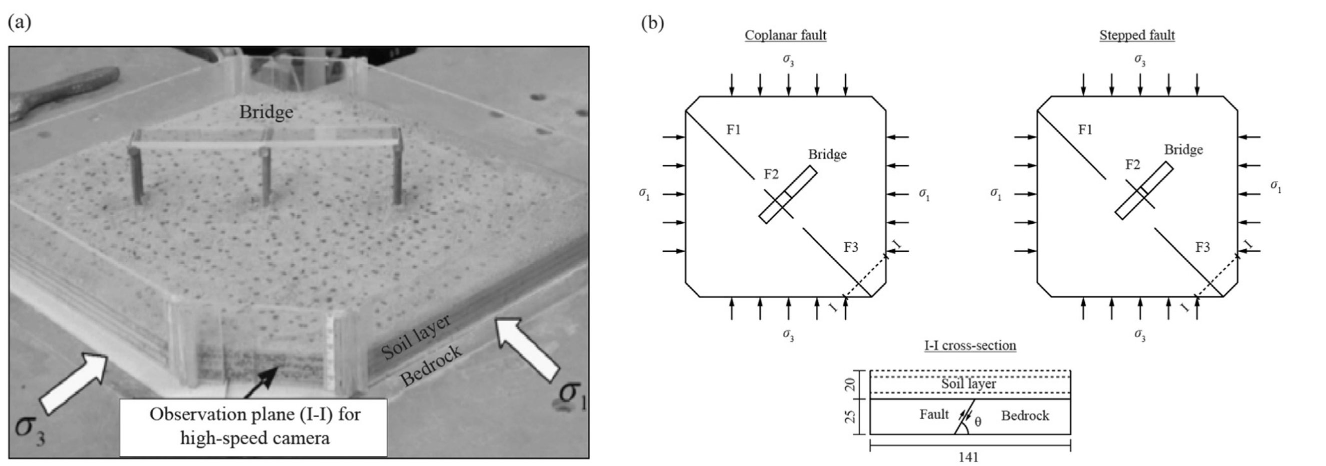

Fig. 17. Experiment of a small-scale (1/250) bridge model subjected to movement of coplanar and stepped buried reverse faults: (a) experimental setup; (b) schematic of bridge model crossing fault (Note: I-I cross section denotes the observation plane for high-speed camera) (Fig. 17a is modified from Wong et al. [135]; Fig. 17b is generated based on information provided by Wong et al. [135]).

rupture zone are: (1) unawareness of the existence of an active fault within the bridge domain during the design and construction of the bridge (e.g., San Diego-Coronado Bay Bridge crossing the Rose Canyon Fault [25], Vincent Thomas Bridge crossing the Palos Verdes Fault [60]); and (2) practical considerations, such as topographic constraints, construction cost, and environmental impact, that dictate the design and construction of the bridge across an already known active fault (e.g., Puqian Approach Bridge in China [51,110], Mercureaux Viaduct in France [80], Thorndon Overbridge in New Zealand [55], I-215/SR-210 interchange project in San Bernardino, California [39]).

Although it is widely recommended to avoid building a bridge across a fault, it is not always possible to achieve this objective, especially in regions with a dense network of active faults. For example, it has been estimated that more than 5% of all bridges in California may either cross faults or lie in the immediate vicinity of fault rupture zones [43]. In that regard, Caltrans has recently embarked on a comprehensive effort to assess the vulnerability of its bridge inventory to geologic hazards such as fault rupture [114]. So far, 268 bridges have been identified within the Alquist-Priolo Earthquake Fault Zones or near unzoned faults capable of surface rupture [19]. Both deterministic [133,47,48] and probabilistic [3,91,99] fault displacement hazard analyses were performed to estimate the potential fault offset at each bridge site. The estimated fault offsets showed that 141 out of the 268 bridges had deterministic or probabilistic potential offsets of more than ~0.12 m (0.4 ft) and up to ~10 m (33 ft) [19], and were characterized as bridges crossing potentially active faults.

The authors have compiled a database of well-documented cases of bridges crossing potentially active fault rupture zones based on information reported in the literature. This database, which is presented in Table 2 and is by no means complete, is dominated by Caltrans bridges, but also includes bridges from China, France, Greece, and New Zealand.[2] It is anticipated that this database will expand considerably as systematic investigations – similar to the one conducted by Sojourner et al. [114] – are carried out in earthquake-prone regions of the world.

[2] A few additional cases of bridges crossing potentially active fault rupture zones have been reported in the literature (e.g., highway bridge in Beppu, Japan [123] and road bridge in the island of Rhodes, Greece [5]), but are not listed in Table 2 due to insufficient information.

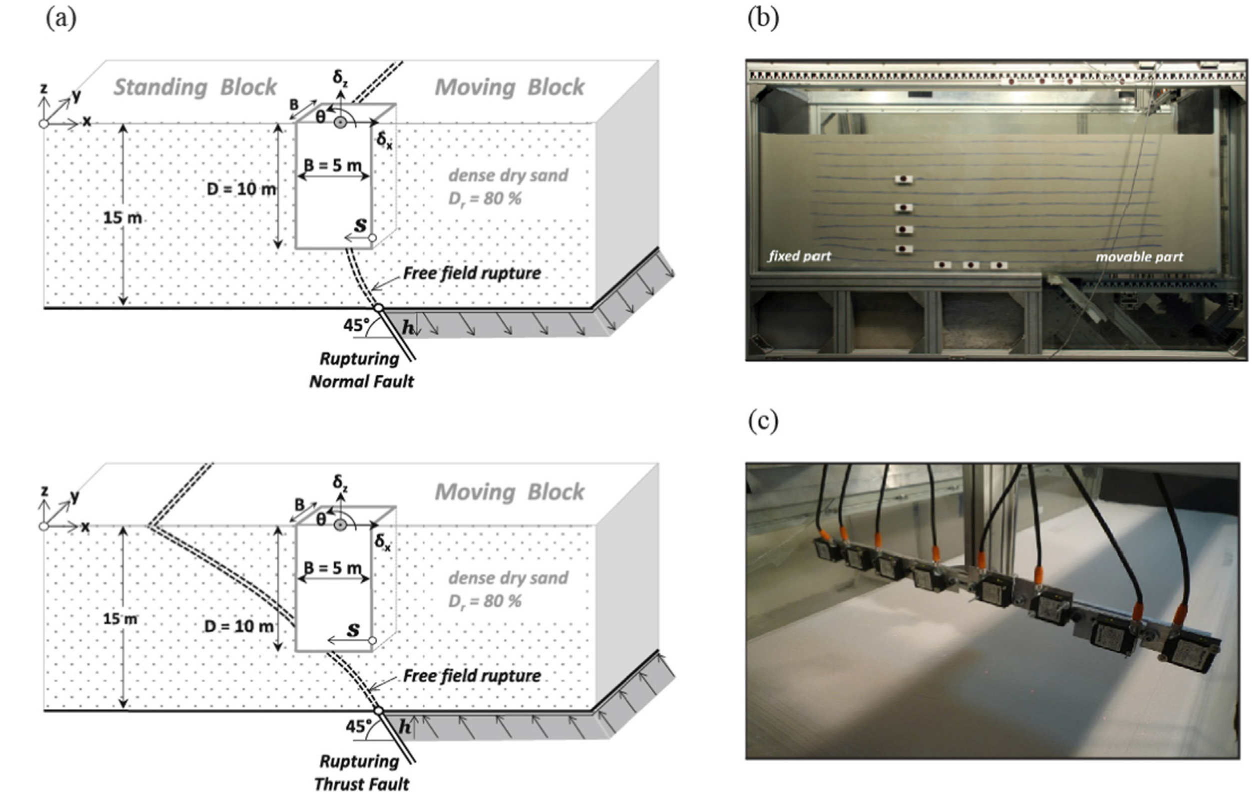

Fig. 18. Experiment of a small-scale (1/20) bridge-pier caisson foundation subjected to dip-slip (normal or reverse) faulting: (a) basic parameters and dimensions at prototype scale; (b) fault rupture box used for experiments; (c) moving row of laser displacement transducers used for scanning the deformed ground surface (all figures are reprinted from Gazetas et al. [35]).

4. Experimental studies

4.1. Small-scale experiments

Murono et al. [92] examined a miniature (1/50 scale) bridge model subjected to surface fault rupture by using a testing device which consisted of two 1300 mm × 650 mm aluminum plates with one plate movable and the other plate fixed (Fig. 16a). The movable plate could shift in the horizontal direction to simulate surface fault dislocation. The piers and girders of the bridge were made of acrylic resin. The bottom of each pier was fixed on the aluminum plates, whereas each girder was supported by four stoppers (i.e., short rubber columns with diameter of 5 mm; see inset in Fig. 16a) arranged on the pier. An image processing system, which consisted of a charge-coupled device camera, an image capturing board and image analysis software, was used in the experiment. Target points were marked on the girders to monitor their movement during the test using the image processing system. Four bridge configurations – corresponding to different combinations of girder lengths (400, 800 and 1200 mm) and number of spans (3, 5, and 7) – along with five fault crossing angles (θ = 30, 60, 90, 120, 150°) were considered in the experiment (Fig. 16b). The test results showed that the fault crossing angle strongly affected the mechanism of fault-induced damage. For $\theta < 90°$, the girder above the fault crossing location fell off the pier(s) without, however, causing any damage to the stoppers of the remaining girders. For $\theta > 90°$, girders away from the fault crossing location fell off the pier(s) and damage was observed in all stoppers due to collision between girders. When $\theta = 90°$, no girders collapsed. For the first two cases, the allowable limit ground displacement to prevent girders from falling off the piers increased as the crossing angle became closer to 90°. Therefore, it was concluded that a fault crossing angle of 90° was the least harmful fault crossing scenario for the bridge configurations considered in the experimental study. Finally, it was found that the allowable limit ground displacement decreased as the girder length increased, suggesting that adoption of longer girders in the design might not be an effective countermeasure for fault-crossing bridges.

Wong et al. [135] studied the relationship between the movement of coplanar and stepped buried reverse faults and the surface fault rupture appearing in a soil layer by using a geomechanical model, which consisted of bedrock, a soil layer, and fault planes. A miniature (1/250 scale) 2-span bridge model was also considered in the experiment to study the correlation between fault movement and observed damage modes. Fig. 17a shows the experimental setup, whereas Fig. 17b displays the test cases of coplanar and stepped buried reverse faults. The coplanar fault system consisted of three discontinuous segments (F1, F2 and F3; see Fig. 17b) lying on the same plane, whereas the stepped fault system was comprised of three discontinuous segments (F1, F2 and F3; see Fig. 17b) with F1 and F3 lying on the same plane and F2 lying on a parallel plane. A biaxial loading system was used to conduct the experiment by simultaneously applying load to the bedrock in two orthogonal horizontal directions, as shown in Fig. 17a and b. The lateral stress σ_3 remained constant after reaching a value of 0.3 MPa, while the lateral stress σ_1 was kept increasing at the same rate until the bridge model failed. The digital speckle correlation method and a high-speed camera were used to observe and analyze the process of fault movement. The results indicated that the failure process for both the coplanar and stepped reverse faults could be divided into four stages: elastic, coalescence, sliding, and failure. The response of the bridge model was negligible during the elastic and coalescence stages. However, the pier closest to the fault tilted toward the footwall during the sliding stage and moved upward and tilted significantly during the failure stage, resulting in the collapse of a span. Furthermore, Wong et al. [135] reported that (1) uplift was greater for the bedrock than for the soil layer; (2) a larger dip angle would result in wider surface fault rupture zone and greater uplift of the hanging wall; and (3) the width of the surface fault rupture zone and the uplift of the hanging wall were greater for the coplanar fault system than for the stepped fault system.

Gazetas et al. [35] explored the key mechanisms affecting the response of a bridge-pier caisson foundation subjected to dip-slip (normal or reverse) faulting. A series of small-scale (1/20) physical model tests were conducted to investigate the response of a square in plan reinforced concrete caisson foundation of prototype dimensions $5\,\text{m} \times 5\,\text{m} \times 10\,\text{m}$, fully embedded in a 15-m deep layer of dry dense sand. The bedrock was subjected to tectonic dislocation due to a 45° dip-slip (normal or reverse) fault with a vertical offset h (Fig. 18a). The tests were conducted in a fault rupture box equipped with a fixed and a movable part, which would simulate normal or reverse faulting by moving downward or upward (Fig. 18b). The fault offset h was imposed slowly in small consecutive increments. After each increment, a high-resolution digital camera was used to photograph the deformed physical model, and the digital images were then processed using the particle image velocimetry technique to compute the caisson displacements and the soil deformation. In addition, a moving row of 8 laser displacement transducers (Fig. 18c) was utilized to produce the surface topography of the deformed ground after each increment. The results showed that a fault rupture (whether normal or reverse) propagating into the soil interacted with the rigid caisson foundation producing new failure mechanisms (diversion, bifurcation, and diffusion). The developing failure mechanisms were shown to depend on the type of faulting, the magnitude of the fault offset, and the exact location of the foundation relative to the fault.

4.2. Large-scale experiments

An experimental study of a quarter-scale 2-span reinforced concrete bridge model subjected to fault rupture was conducted at the University of Nevada, Reno by using a shake table system [102]. The bridge model was a continuous, posttensioned reinforced concrete box-girder structure with three double-column piers of varying height. Fig. 19a and b shows the geometry and shake table setup of the bridge model, respectively. The assumed earthquake was generated by a vertical strike-slip fault (oriented in the east-west direction) crossing the bridge model (oriented in the north-south direction) in the middle of the northern span at an angle of 90° (Fig. 19c). This fault crossing angle was selected to maximize the effect of in-plane rotation of the superstructure. The ground motions simulated for each pier included long-period pulses in the fault-normal direction due to rupture directivity and permanent ground displacements in the fault-parallel direction due to earthquake faulting. However, only the fault-parallel motions were applied in the shake table tests; the fault-normal motions were not used because they would run in the longitudinal direction of the bridge, and the bridge model did not include abutment elements to model the longitudinal behavior realistically.

An identical bridge model that had previously been tested under far-field spatially uniform ground motions [59] was utilized for comparison purposes. For the bridge model subjected to fault rupture, the plastic deformation and apparent damage were minimal in the end piers, but severe in the intermediate pier. Conversely, for the identical bridge model subjected to spatially uniform ground motions, the damage in all piers was significant. In addition, it was found that the shortest piers failed when the bridge model was subjected to spatially uniform ground motions, but the tallest piers experienced the severest damage under fault rupture. Finally, torsional cracks were observed in the piers of the bridge model subjected to fault rupture due to significant in-plane rotation of the superstructure, whereas no apparent torsional cracks were observed in the spatially uniform ground motion study.

5. Analytical and numerical studies[3]

5.1. Simplified analysis

Gloyd et al. [39] proposed a simple design approach for estimating the demands of ordinary bridges[4] crossing fault rupture zones by considering two specific load cases in addition to the standard loading defined in design codes in California. This approach was used to design bridges in the I-215/SR-210 interchange project in San Bernardino, California.

Anastasopoulos et al. [5] proposed a two-step methodology for the analysis and design of bridges crossing fault rupture zones (with emphasis on normal faulting). In the first step (local-level analysis), the response of a single bridge pier subjected to fault rupture deformation was analyzed using the finite element software Abaqus [1]. A detailed model was utilized to simulate soil-foundation-structure interaction under fault rupture, with the superstructure modeled in a simplified manner. In the second step (global-level analysis), a detailed model of the superstructure was subjected to the displacements and rotations computed in the first step. Furthermore, a parametric study was conducted to investigate the behavior of typical models of viaducts and overpass bridges founded on piles or caissons. It was concluded that: (1) rupture propagation path was strongly affected by the presence of the foundation; (2) pile foundations were vulnerable to fault rupture deformation, whereas caisson foundations were clearly advantageous; (3) fault crossing location played an important role in the response of the bridge; and (4) statically-indeterminate superstructures were vulnerable to fault rupture deformation, whereas statically-determinate superstructures were insensitive. Finally, an application of the proposed method was presented for a 3-span arched railway bridge in Greece.

Konakli and Der Kiureghian [67] estimated the seismic demands for bridges crossing fault rupture zones within the framework of the multiple-support response spectrum method. A coherency function was developed to describe the variability in the support motions for a bridge crossing a vertical strike-slip fault under the assumptions of stationarity and zero residual slip. The validity of the proposed approach was assessed by analyzing an existing 4-span curved bridge in California for various orientations of the bridge relative to the fault. The response quantities were the relative transverse displacement between the ends of the second span and the shear force in the middle of the same span. Comparisons with results obtained using response history analysis demonstrated the ability of the multiple-support response spectrum method to provide good estimates of the seismic demands.

Goel and Chopra [43] proposed two approximate procedures (response spectrum analysis and linear static analysis) for estimating the peak responses of linearly elastic ordinary bridges crossing fault rupture zones. Goel and Chopra [44] extended these methodologies by proposing three approximate procedures (modal pushover analysis, linear dynamic analysis, and linear static analysis) for estimating the peak responses of ordinary bridges deforming into their inelastic range. These procedures estimated the peak response of the bridge by superposing the peak values of quasi-static and dynamic responses. The accuracy of the proposed procedures was investigated by comparing the estimated peak responses against response history analysis results obtained using the software framework OpenSees [95]. Two scenarios were examined: (1) bridges oriented orthogonal to a vertical strike-slip fault and subjected to fault-parallel ground motions; and (2) bridges oriented orthogonal to a dip-slip fault and subjected to fault-normal ground motions. The response quantities considered were the pier drift

[3] Several analytical and numerical studies on fault-crossing bridges have been published in Japanese (e.g., [122,79,96]), but are not discussed in this section due to the authors' insufficient knowledge of that language.

[4] Caltrans bridges are divided into two categories: ordinary (standard and non-standard) and important [143,18].

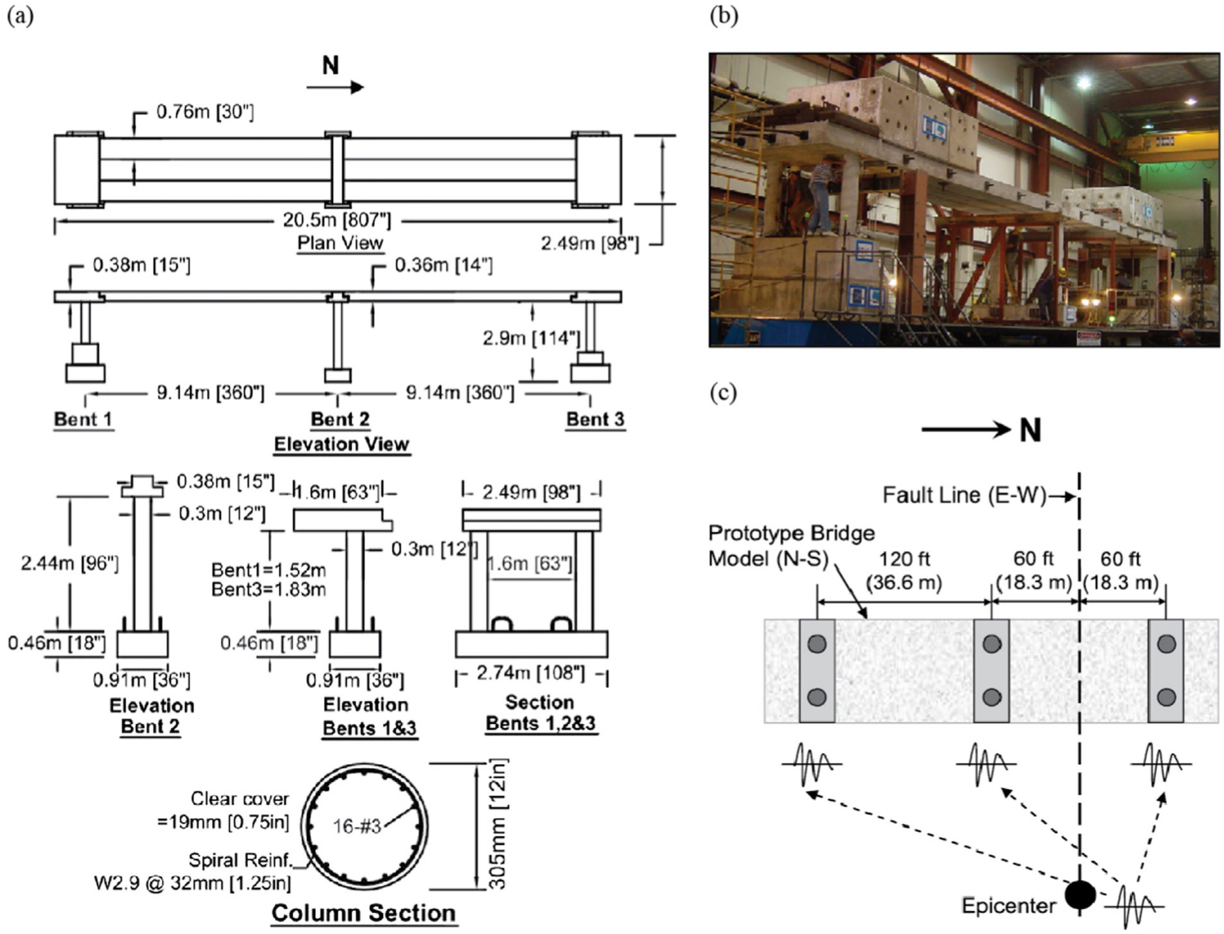

Fig. 19. Experiment of a large-scale (1/4) two-span reinforced concrete bridge model subjected to fault rupture: (a) geometry and column reinforcement; (b) shake table setup; (c) bridge and fault locations for ground motion simulation (all figures are reprinted from Saiidi et al. [102]).

and deck displacement at the abutment. These comparisons demonstrated that the proposed procedures provided estimates of peak response that were close enough to the results obtained from response history analysis.

Saiidi et al. [102] verified the effectiveness of the linear static analysis procedure proposed by Goel and Chopra [43] in estimating the peak relative displacement in the critical pier of their bridge model subjected to fault rupture during a shake table test (see Section 4.2). In particular, Saiidi et al. [102] compared the peak relative displacements of all the piers calculated using the linear static analysis procedure with the measured values obtained from the shake table test and the calculated values obtained from nonlinear response history analysis using OpenSees [95]. The comparison showed that, for the most critical pier of the bridge model, the linear static analysis procedure estimated the peak relative displacement reasonably well.

Goel et al. [41] (see also [40]) extended the linear dynamic analysis procedure proposed by Goel and Chopra [44] to a new method referred to as the fault-rupture response spectrum analysis method, which took into account simultaneous application of fault-parallel and fault-normal ground motions associated with strike-slip faulting. The proposed method was then used for two representative curved bridges in California (along with several angles and locations of fault crossing) to investigate its accuracy against nonlinear response history analysis performed in OpenSees [95]. Comparison results showed that the proposed method provided estimates of peak displacement response that were close enough to the nonlinear response history analysis results in all considered cases.

Shantz et al. [106] developed a method to evaluate fault rupture hazard mitigation for bridges using mitigation efficiency, a parameter defined as the decrease in collapse probability (based on a 75-year design life) divided by the increase in bridge cost. A hypothetical bridge crossing the Hayward Fault (an active strike-slip fault in the San Francisco Bay Area) was considered to illustrate the developed method. In order to compare mitigation efficiency for different levels of design, alternative bridge designs with varying capacity for displacement offset were investigated. For each alternative design, a fragility curve and a cost estimate were developed, and the collapse probability was calculated based on the fragility curve and a simple probabilistic fault-offset model. The mitigation efficiencies for these designs were then calculated and compared with typical mitigation efficiencies associated with implementing Caltrans seismic design criteria for shaking hazard. The results showed that, while designing a bridge to accommodate large fault offset might double costs, the corresponding reduction in collapse probability was significant, leading to mitigation efficiencies twice as large as those obtained in typical design practice for shaking hazard.

Todorovska and Trifunac [121] presented a probabilistic methodology, formulated within the framework of probabilistic seismic hazard analysis, for predicting the peak relative displacement of bridge piers. The simultaneous action of three types of forces was considered: (1) dynamic forces caused by ground shaking; (2) quasi-static forces caused by the transient differential motions of the supports due to wave passage; and (3) static forces caused by permanent displacement across the fault from seismic slip. The output of the analysis consisted of uniform hazard relative displacement spectra for piers for a given probability of exceedance during a specified exposure period. The proposed methodology was then used for three sites in southern

California and the relative significance of each type of force (dynamic, quasi-static, and static) was analyzed. Among other findings, Todorovska and Trifunac [121] reported that the fault displacement dominated the hazard only for very small probabilities of exceedance.

Gazetas et al. [35] studied the response of a bridge-pier caisson foundation subjected to dip-slip (normal or reverse) faulting using a three-dimensional finite element model built in Abaqus [1] accounting for soil strain-softening. The dimensions of the finite element model were equal to those of the fault rupture box used in the experiments conducted by Gazetas et al. [35] (see Section 4.1). The bottom boundary of the finite element model was split in two parts: one part (footwall) remained stationary and the other (hanging wall) moved upward or downward to simulate reverse or normal faulting. The fault dislocation was applied to the moving block in small quasi-static analysis increments. Similar to the physical model tests, the numerical simulations examined the effects of faulting type, magnitude of fault offset, and caisson's position relative to the fault rupture on the mechanisms affecting the response of the caisson foundation. Overall, the numerical results were in good agreement with the experimental observations, although they could not always capture the detailed strain localizations observed in the experiments. The discrepancies between numerical and experimental results were primarily attributed to the unavoidable small-scale effects. Nevertheless, the predicted translational and rotational displacements of the caisson top were in accord with the experiments.

5.2. Response history analysis

Park et al. [98], Ucak et al. [124], and Yang et al. [141] investigated the seismic response of a typical 10-span segment of Bolu Viaduct 1 – a seismically isolated bridge traversed by the North Anatolian Fault during the 1999 M_w 7.2 Duzce earthquake (see Section 2.4) – using nonlinear response history analysis and spatially varying seismic excitations selected using different techniques. The finite element model of the 10-span segment was built in SAP2000 [103] by Park et al. [98] and in Abaqus [1] by Ucak et al. [124] and Yang et al. [141]. Park et al. [98] reported that the relative displacement between the superstructure and the piers of the viaduct exceeded the capacity of the seismic isolation system at an early stage of the ground shaking and the shear keys played a critical role in preventing the superstructure from falling off the pier caps. Ucak et al. [124] studied the behavior of the 10-span segment of Bolu Viaduct 1 subjected to strong ground shaking with and without fault crossing considerations. Two seismic isolation systems, the original design (consisting of sliding pot bearings along with steel yielding devices) and a potential retrofit design (consisting of friction pendulum bearings), were considered in the analysis. For both seismic isolation systems, the isolation displacement demands for the fault crossing case were almost twice as much as those for the non-fault crossing case, whereas the pier drift demands were comparable in both cases. The results also demonstrated that the fault crossing location and fault crossing angle substantially influenced the isolation displacement and pier drift demands of the bridge. Moreover, the isolation permanent displacement demands were greatly influenced by the restoring force capability of the considered seismic isolation systems, when fault crossing effects in the excitations were ignored. In the case of fault crossing, the isolation permanent displacement demands of both isolation systems were dominated by the substantial permanent ground displacement along the fault trace imposed upon the bridge. Finally, Yang et al. [141] investigated the effect of ground motion filtering on the seismic response of the 10-span segment of Bolu Viaduct 1 with and without fault crossing considerations. To accomplish this objective, a near-fault ground motion record from the 1992 M_w 7.2 Landers earthquake – processed with and without high-pass filtering – was used in the analysis. For the non-fault-crossing bridge, the utilization of the high-pass filtered ground motion led to underestimating the demands of pier top, pier bottom and deck displacements. However, the demands of isolation displacement, isolation permanent displacement and pier drift were almost identical for both the unfiltered and filtered versions of the ground motion record. On the other hand, for the fault-crossing bridge, all response quantities were significantly underestimated when the high-pass filtered ground motion was used.

Goel and Chopra [42] utilized nonlinear response history analysis to examine the seismic demands of ordinary bridges subjected to spatially uniform and spatially varying ground motions for three shear-key conditions (nonlinear, elastic, and no shear keys) at the abutments. The finite element models of the analyzed bridges were built in OpenSees [95]. It was concluded that the seismic demands of a bridge with nonlinear shear keys could generally be bounded by the demands of the bridge with the other two shear-key conditions (elastic shear keys and no shear keys) for both types of ground motions. For a bridge subjected to spatially uniform ground motions, shear keys might be ignored in estimating an upper bound value of seismic demands. However, for a bridge crossing a fault rupture zone, analysis for two shear-key cases (no shear keys and elastic shear keys) was required for estimating the upper bound values of seismic demands.

Luo and Li [76] adopted the response spectrum analysis procedure proposed by Goel and Chopra [43] and linear response history analysis performed in SAP2000 [103] to investigate the seismic response of a cable-stayed bridge crossing a strike-slip fault. Their study indicated that both methods yielded very similar results in terms of maximum displacements and internal forces at critical locations/cross-sections of the bridge. In addition, it was found that the shear forces and bending moments at the bottom of certain piers were reduced when the transverse restraints between the piers and the superstructure were removed. Finally, it was reported that the seismic response of the bridge was significantly underestimated when fault crossing was ignored.

Yang and Li [140] utilized nonlinear response history analysis to investigate the response of a 6-span, simply-supported bridge equipped with lead rubber or pot bearings subjected to ground shaking with and without fault crossing considerations. The results showed that lead rubber bearings were more effective than pot bearings in reducing the seismic response of the bridge and that the seismic response was greatly underestimated when fault crossing was ignored.

Hui [53] adopted nonlinear response history analysis to investigate the effects of fault crossing angle, fault crossing location, pier height, and bearing type on the seismic response of bridges crossing strike-slip faults. In that investigation, three continuous bridges (with two, three and five spans) were considered, and their finite element models were built in OpenSees [95]. The response quantities of interest included the maximum bending moment and torque at the pier top and bottom, the maximum and permanent bearing deformations, and the maximum and permanent pier drifts. The analysis results showed that: (1) most response quantities were significantly underestimated when fault crossing was ignored; (2) the maximum bending moment at the pier bottom, as well as the maximum and permanent bearing deformations increased when the fault crossing location shifted from the middle span to the end span; (3) all response quantities attained their minimum values for a fault crossing angle of 90°; (4) bridges with a fixed combination, yet varying distributions, of pier heights experienced similar maximum and permanent bearing deformations, but significantly different maximum bending moments and torques at the pier bottom; (5) for bridges with uniform pier height, all response quantities increased with increasing pier height; and (6) the maximum bending moment and torque at the pier bottom were significantly larger for the bridge equipped with pot bearings than for the bridge with lead rubber bearings.

Zeng [148] investigated the seismic response of a deep-water cable-stayed bridge crossing a strike-slip fault using nonlinear response history analysis. The finite element model of the analyzed bridge was built in OpenSees [95]. Different earthquake magnitudes, water depths, fault crossing angles, and fault crossing locations were considered in the analysis. For various earthquake magnitudes, the maximum bending moment and shear force occurred at the bottom of the main tower, whereas the maximum displacement appeared at the tower top or at the cable anchorage zone. Furthermore, it was observed that the seismic response of the main tower increased with increasing water depth and its damage was aggravated when the water depth reached a certain height (i.e., pile cap in the analyzed cable-stayed bridge), thus suggesting that the impact of the surrounding water should be considered. The results also showed that the fault crossing angle and the fault crossing location had significant influence on the seismic response of the bridge. It was concluded that the most favorable scenario was that of a cable-stayed bridge crossing the strike-slip fault over a simply-supported span at an angle of 90°.

In a recent study, Wu et al. [137] utilized linear response history analysis to investigate the seismic response of a 4-span bridge crossing a hypothetical reverse fault. Their results indicated that the spatially varying ground motions caused significant differences in the velocity and displacement time-history responses of all masses lumped at the pier tops. In addition, it was found that the displacement responses resulted in residual offsets.

6. Seismic design provisions and recommendations

The Alquist-Priolo Earthquake Fault Zoning (AP) Act – a California state law passed in 1972 as a result of the destructive 1971 M_w 6.6 San Fernando earthquake – is probably the earliest provision for structures crossing active faults. The intent of the AP Act is to ensure public safety by prohibiting the siting of most structures for human occupancy across traces of active faults that constitute a potential hazard to structures from surface faulting or fault creep [13]. The AP Act requires the State Geologist (California Geological Survey) to issue maps delineating regulatory zones (known as earthquake fault zones) around traces of active faults and the lead agencies affected by the zones to regulate development projects within the earthquake fault zones. According to the AP Act, a structure for human occupancy cannot be built over the trace of an active fault and must be set back from the fault trace generally at least 15 m (50 ft) [14].

A Caltrans Bridge Memo to Designers [16] – which serves as a supplement to the AASHTO Specifications [4] and the Caltrans Seismic Design Criteria [18] – presents a simplified analysis procedure, in lieu of nonlinear response history analysis, for ordinary bridges that cross strike-slip faults. The response of interest is the relative displacement between the top and bottom of the piers and between the superstructure and the abutment seats. The steps of the simplified analysis procedure are as follows: (1) obtain the design fault offset and ground shaking hazard for the bridge site; (2) obtain the quasi-static response of the structure due to the design fault offset; (3) obtain the dynamic response of the structure; (4) combine the static and dynamic response to obtain the seismic demand; and (5) perform a pushover analysis at each bent to obtain the seismic capacity. Step 1 requires the estimation of the design fault offset based on the larger of the probabilistic or deterministic offset or a site-specific offset. Step 2 computes the quasi-static response of the bridge by applying both gravity loads and foundation offsets to a nonlinear bridge model. Step 3 is based on the linear dynamic analysis and linear static analysis procedures proposed by Goel and Chopra [44] for estimating the dynamic response of nonlinear bridges crossing fault rupture zones. Finally, Step 5 is performed to ensure that the displacement capacity is greater than the displacement demand.

In addition, Caltrans requires preliminary investigation of fault rupture hazard to identify active surface faults that may cross beneath a bridge [17,18,20]. Specifically, the Caltrans Seismic Design Criteria [18] require Geotechnical Service to provide the following recommendations: (1) location and orientation of fault traces or zones with respect to structures; (2) expected horizontal and vertical displacements; (3) description of additional evaluations or investigations that could refine the above information; and (4) strategies to address ground rupture including avoidance (preferred) and structural design. According to a Caltrans Bridge Memo to Designers [17] and the Caltrans Geotechnical Manual [20], if any portion of the bridge structure falls within an Alquist-Priolo Earthquake Fault Zone or within ~300 m (1000 ft) of an unzoned active fault, surface fault rupture displacement hazard analysis should be conducted. This includes a more in-depth literature review, site reconnaissance, geological mapping, and fault trench excavation to accurately locate and age-date the fault and/or splays with respect to the bridge. When there is a confirmed fault rupture hazard, both deterministic and probabilistic fault displacement hazard analyses must be performed to determine the magnitude and direction of the anticipated surface displacement along the fault. The design fault offset is based on the larger of the deterministic or probabilistic displacement hazard values.

In China, the Code for Seismic Design of Railway Engineering [83] recommends adoption of a simply-supported design with short span lengths and pier heights, when it is unavoidable to build a bridge over a seismogenic fault. In this case, the code also specifies that the foundations of piers and abutments should not be arranged within the fault rupture zone. Furthermore, the Guidelines for Seismic Design of Highway Bridges [85] and the Code for Seismic Design of Urban Bridges [84] contain detailed provisions for the design of bridges in the vicinity of seismogenic faults. According to these provisions, which are presumably applicable both to non-fault crossing and fault crossing conditions, the effects of fault offset on bridges can be neglected when any of the following conditions is satisfied: (1) the seismic fortification intensity (generally defined as the seismic intensity with a 10% probability of exceedance in 50 years) is less than 8; (2) the fault is not a Holocene active fault; and (3) the depth of soil overlying a bedrock fault is greater than 60 m (respectively, 90 m) for regions with a seismic fortification intensity of 8 (respectively, 9). If none of the above conditions is satisfied, the following measures should be adopted: (1) bridges in category A (with a span length greater than 150 m) should be constructed sufficiently far away from primary fault rupture zones; i.e., distances between piers and primary fault rupture zone should be greater than 300 m (respectively, 500 m) for regions with a seismic fortification intensity of 8 (respectively, 9); (2) bridges in categories B, C, and D (with span lengths less than 150 m) should adopt designs with short span lengths to facilitate repair in the event of a destructive earthquake; and (3) when it is unavoidable to build a bridge in the immediate vicinity of a seismogenic fault, all piers and abutments should preferably be arranged on the same side of the fault (footwall is recommended). Finally, the Specification of Seismic Design for Highway Engineering [86] states that the layout of a highway route – a term that includes roads, bridges, and tunnels – should be constructed far away from a seismogenic fault rupture zone. When it is unavoidable to cross the fault, the highway route should preferably be laid out over a relative narrow zone of the fault.

In Europe, according to Eurocode 7-1 [27], the design of spread foundations on rock shall consider the presence of weak layers, such as solution features or fault zones, beneath the foundation. Furthermore, Eurocode 8-5 [29] has provisions on the proximity of structures (i.e., buildings, bridges, towers, masts, chimneys, silos, tanks, and pipelines) to seismically active faults: (1) buildings of importance classes II, III, IV defined in Eurocode 8-1 [28] shall not be erected in the immediate vicinity of tectonic faults recognized as being seismically active in official documents issued by competent national authorities; (2) an absence of movement in the Late Quaternary may be used to identify inactive faults for most structures which are not critical for public safety; and (3) special geological investigations shall be carried out for urban planning purposes and for important structures to be erected near potentially active faults in areas of high seismicity in order to determine the ensuing hazard in terms of ground rupture and the severity of ground shaking.

In New Zealand, the Bridge Manual [94] specifies that the design of any structure located in an area that is over an active fault with a recurrence interval of 2000 years or less shall recognize the large movements which may result from settlement, rotation or translation of substructures. To the extent practical and economic, and taking into consideration possible social consequences, measures shall be incorporated to mitigate against these effects.

7. Summary, concluding remarks, and future directions

This article presented a comprehensive review of case studies, experimental, analytical and numerical investigations, and seismic design provisions and recommendations related to fault-crossing bridges. The main contributions of this article are summarized as follows:

1. Detailed information about fault-crossing bridges damaged in past earthquakes was collected from the literature and compiled in a database presented in Section 2, including description of bridges, damaging earthquakes, fault crossing conditions and observed damage modes, as well as a comprehensive list of references.
2. A database of well-documented cases of bridges crossing potentially active fault rupture zones was compiled in Section 3 based on information provided in the literature. This database is dominated by bridges in California, but also includes bridges from China, France, Greece, and New Zealand.
3. A limited number of small- and large-scale experimental studies have been conducted to investigate the seismic response of bridges crossing fault rupture zones. The research findings of these studies – which were summarized in Section 4 – demonstrate that bridges may suffer significant damage due to surface fault rupture.
4. Simplified methods proposed in the literature for the analysis and design of bridges subjected to fault crossing were reviewed in Section 5.1. Several of these methods have been validated to provide estimates of seismic demands that are close enough to the results obtained from response history analysis and experimental studies.
5. Response history analysis has extensively been used in past studies to investigate the seismic response of different types of bridges crossing fault rupture zones. The research findings of these studies – which were summarized in Section 5.2 – demonstrate that the seismic response of fault-crossing bridges is affected by various parameters, including earthquake magnitude, fault crossing angle, fault crossing location, pier height, bearing type, shear-key condition, and water depth (for deep-water bridges). In addition, ground motion filtering may also have a significant effect on the computed seismic response of fault-crossing bridges.
6. As discussed in Section 6, only a few seismic design codes have established provisions and recommendations for the analysis and design of bridges crossing fault rupture zones. In the United States, Caltrans has proposed a simplified procedure – which serves as a supplement to the AASHTO Specifications and the Caltrans Seismic Design Criteria – for ordinary bridges crossing strike-slip faults. In addition, Caltrans requires investigation of fault rupture hazard to identify active surface faults that may cross beneath a bridge. In China, seismic design provisions and recommendations have also been proposed for the analysis and design of fault-crossing bridges. Finally, only generic provisions and recommendations are outlined in seismic design codes in Europe and New Zealand.

Based on findings reported and advances achieved in past studies, the following significant problems have been identified as requiring further investigation:

1. A major challenge in studying the seismic response of fault-crossing bridges is the selection of appropriate input ground motions. To date, actual ground motions have rarely been recorded on both sides of and in close proximity to the surface fault rupture. As a result, researchers typically estimate ground motions across the fault rupture using different simulation approaches. However, the simulation of ground motions in the immediate vicinity of the fault is still an open problem and further research is required.
2. Past studies have primarily focused on bridge structures crossing strike-slip faults, whereas the response of bridges traversed by dip-slip faults has not sufficiently been investigated. Specifically, parametric studies using response history analysis should be conducted to examine the effect of different parameters (e.g., earthquake magnitude, fault crossing angle, fault crossing location, pier height, bearing type, shear-key condition, and water depth) on the seismic response of bridges crossing dip-slip faults. In addition, the influence of dip angle, hanging wall effect and vertical ground motion – parameters that are particularly important for dip-slip faults – should also be examined. Finally, large-scale experimental studies of bridges crossing dip-slip faults, though technically challenging, could also provide useful insights into the problem under investigation.
3. Past earthquakes have clearly demonstrated the vulnerability of bridges crossing fault rupture zones, thus suggesting that conventional design methods do not provide the desired performance levels. However, the seismic design codes of most earthquake-prone countries either ignore the effect of surface fault rupture on bridges or recommend prevention of bridge construction across a fault. Even the simplified analysis procedure proposed by Caltrans – which is perhaps the most comprehensive approach incorporated in seismic design codes – applies only to ordinary bridges crossing strike-slip faults. Therefore, there is a clear need to establish provisions and recommendations for the analysis, design and retrofit of different types of bridges (e.g., ordinary and important; isolated and non-isolated; short-, medium- and long-span; slab, beam, truss, arch, cable-stayed and suspension; simply-supported, continuous and cantilever) crossing fault rupture zones of strike-slip and dip-slip earthquakes. This will enable future bridges to withstand the effects of fault crossing and will ensure the functionality of existing bridges against surface fault rupture.

Acknowledgments

The authors would like to acknowledge partial financial support provided by the U.S. National Science Foundation under Grant No. CMMI-1360734.

References

[1] ABAQUS. ⟨https://www.3ds.com/products-services/simulia/products/abaqus/⟩, [Mar. 13, 2018].
[2] Abe M, Kosa K, Unjoh S, Takahashi Y, Machida A, Maruyama K, et al. Chapter 4: damage to transportation facilities. In: The 1999 Ji-Ji earthquake, Taiwan – investigation into the damage to civil engineering structures. Tokyo, Japan: Japan Society of Civil Engineers; 1999, p. 1–40.
[3] Abrahamson N. Appendix C: probabilistic fault rupture hazard analysis. In: General seismic requirements for the design on new facilities and upgrade of existing facilities. San Francisco, CA: San Francisco Public Utilities Commission; 2008.
[4] American Association of State Highway and Transportation Officials (AASHTO). AASHTO LRFD bridge design specifications, 6th edition. Washington, DC; 2012.
[5] Anastasopoulos I, Gazetas G, Drosos V, Georgarakos T, Kourkoulis R. Design of bridges against large tectonic deformation. Earthq Eng Eng Vib 2008;7(4):345–68.
[6] Ashley M, Dougherty B, Jones RM, Kompfner TA, Pourvahidi S. Holding steady. Civ Eng 2001;71(7):52–7. 85.
[7] Aydan O. Actual observations and numerical simulations of surface fault ruptures and their effects on engineering structures. In: Proceedings of the 8th U.S.-Japan workshop on earthquake resistant design of lifeline facilities and countermeasures against liquefaction, Technical Report MCEER-03-0003. Buffalo, NY: Multidisciplinary Center for Earthquake Engineering Research; 2003, p. 227–37.
[8] Aydan O, et al. A reconnaissance report on 2008 Wenchuan earthquake. Tokyo, Japan: Japan Society of Civil Engineers; 2008.
[9] Baker G, Ingham T, Heathcote D. Seismic retrofit of Vincent Thomas suspension bridge. Transp Res Rec 1998;1624:64–72.
[10] Behr J, Bilham R, Bodin P, Burford RO, Burgmann R. Aseismic slip on the San Andreas fault south of Loma Prieta. Geophys Res Lett 1990;17(9):1445–8.
[11] Billings IJ, Powell AJ. Thorndon Overbridge seismic retrofit. In: Proceedings of the 11th world conference on earthquake engineering. Acapulco, Mexico; 1996, Paper No. 1477.
[12] Bray JD. Developing mitigation measures for the hazards associated with earthquake surface fault rupture. In: Proceedings of the 1st workshop on seismic fault-

induced failures – possible remedies for damage to Urban facilities. Tokyo, Japan: University of Tokyo Press; 2001, p. 55–79.
[13] Bryant WA. History of the Alquist-Priolo earthquake fault zoning act, California, USA. Environ Eng Geosci 2010;16(1):7–18.
[14] Bryant WA, Hart EW. Fault-rupture hazard zones in California: Alquist-Priolo Earthquake Fault Zoning Act with index to earthquake fault zones maps. Special Publication 42. Sacramento, CA: Department of Conservation, California Geological Survey; 2007.
[15] Buckle IG, Chang K-C. Section 6: performance of highway bridges. In: The Chi-Chi, Taiwan, earthquake of september 21, 1999: reconnaissance report, Technical Report MCEER-00-0003. Buffalo, NY: Multidisciplinary Center for Earthquake Engineering Research; 2000, p. 65–86.
[16] California Department of Transportation (Caltrans). Bridge memo to designers 20-8: analysis of ordinary bridges that cross faults. Sacramento, CA; 2013.
[17] California Department of Transportation (Caltrans). Bridge memo to designers 20-10: fault rupture. Sacramento, CA; 2013.
[18] California Department of Transportation (Caltrans). Seismic design criteria, Version 1.7. Sacramento, CA; 2013.
[19] California Department of Transportation (Caltrans). Fault rupture. 〈http://www.dot.ca.gov/hq/esc/geotech/geo_support/geo_instrumentation/fault_rupture/〉, [Oct. 27, 2017].
[20] California Department of Transportation (Caltrans). Geotechnical Manual. Sacramento, CA; 2017.
[21] Chang K-C, Chang D-W, Tsai M-H, Sung Y-C. Seismic performance of highway bridges. Earthq Eng Eng Seismol 2000;2(1):55–77.
[22] Chen C-H, Chou H-S, Yang C-Y, Shieh B-J, Kao Y-H. Chelungpu fault inflicted damages of pile foundations on FWY route 3 and fault zoning regulations in Taiwan. In: Proceedings of the 2nd workshop on seismic fault-induced failures-possible remedies for damage to urban facilities. Tokyo, Japan: University of Tokyo Press; 2003, p. 1–19.
[23] Christopoulos C, Lopez-Garcia D, Tsai K-C. Educational reconnaissance of the area affected by the 1999 Chi-Chi earthquake – three years later. Earthq Spectra 2005;21(1):31–52.
[24] Ciotoli G, Lombardi S, Annunziatellis A. Geostatistical analysis of soil gas data in a high seismic intermontane basin: Fucino Plain, central Italy. J Geophys Res 2007;112:B05407. https://doi.org/10.1029/2005JB004044.
[25] Dameron RA, Sobash VP, Lam IP. Nonlinear seismic analysis of bridge structures. Foundation-soil representation and ground motion input. Comput Struct 1997;64(5/6):1251–69.
[26] Erdik M, Aydinoglu N, Uckan E, Celep U, Apaydin N. The 1999 Turkey earthquakes: bridge performance and remedial actions. Learning from earthquake series IV. Oakland, CA: Earthquake Engineering Research Institute; 2003.
[27] European Committee for Standardization (CEN). Eurocode 7: geotechnical design – Part 1: General rules. Brussels, Belgium; 2004.
[28] European Committee for Standardization (CEN). Eurocode 8: design of structures for earthquake resistance – Part 1: general rules, seismic actions and rules for buildings. Brussels, Belgium; 2004.
[29] European Committee for Standardization (CEN). Eurocode 8: design of structures for earthquake resistance – Part 5: foundations, retaining structures and geotechnical aspects. Brussels, Belgium; 2004.
[30] Faccioli E, Anastasopoulos I, Gazetas G, Callerio A, Paolucci R. Fault rupture–-foundation interaction: selected case histories. Bull Earthq Eng 2008;6(4):557–83.
[31] Faccioli E, Paolucci R, Pessina V. Engineering assessment of seismic hazard and long period ground motions at the Bolu Viaduct site following the November 1999 earthquake. J Seismol 2002;6(3):307–27.
[32] Fan Q-W, Qian Y-J, Feng Z-X. Seismic collapse analysis for Xiaoyudong Bridge axial-shear-flexural interaction. In: Proceedings of the 15th world conference on earthquake engineering. Lisbon, Portugal; 2012, p. 10030–9.
[33] Federal Highway Administration (FHWA). National bridge inventory (NBI); 2016. 〈http://www.fhwa.dot.gov/bridge/nbi/ascii.cfm〉, [Oct. 22, 2017].
[34] Fenves GL, Mahin SA. Summary of performance of modern bridges in the 1999 Chi-Chi, Taiwan earthquake. In: Proceedings of the workshop on instrumental systems for diagnostics of seismic response of bridges and dams. Richmond, CA: Consortium of Organizations for Strong-Motion Observation Systems; 2001, p. 77–87.
[35] Gazetas G, Zarzouras O, Drosos V, Anastasopoulos I. Bridge-pier caisson foundations subjected to normal and thrust faulting: physical experiments versus numerical analysis. Meccanica 2015;50(2):341–54.
[36] Gelagoti F. Estimation of strong motion experienced in the vicinity of the Bolu Viaduct during the 1999 Duzce earthquake: development and validation of a hybrid method. Bull Seismol Soc Am 2014;104(2):720–40.
[37] Ghasemi H, Cooper JD, Imbsen R, Piskin H, Inal F, Tiras A. The November 1999 Duzce earthquake: post-earthquake investigation of the structures on the TEM. Publication No. FHWA-RD-00-146. Washington, DC: Federal Highway Administration; 2000.
[38] Gillies AG, Anderson DL, Mitchell D, Tinawi R, Saatcioglu M, Gardner NJ, et al. The August 17, 1999, Kocaeli (Turkey) earthquake – lifelines and preparedness. Can J Civ Eng 2001;28:881–90.
[39] Gloyd S, Fares R, Sánchez A, Trinh V. Designing ordinary bridges for ground fault rupture. In: Proceedings of the 3rd national seismic conference and workshop on bridges and highways, Technical Report MCEER-02-SP04. Buffalo, NY: Multidisciplinary Center for Earthquake Engineering Research; 2002, p. 149–161.
[40] Goel R, Qu B, Rodriguez O, Tures J. Bridge design for earthquake fault crossings: synthesis of design issues and strategies, Report to CALTRANS, No. CP/SEAM-2012/01. San Luis Obispo, CA: California Polytechnic State University; 2012.
[41] Goel R, Qu B, Tures J, Rodriguez O. Validation of fault rupture-response spectrum analysis method for curved bridges crossing strike-slip fault rupture zones. J Bridge Eng-ASCE 2014;19(5):06014002. https://doi.org/10.1061/(ASCE)BE.1943-5592.0000602.
[42] Goel RK, Chopra AK. Role of shear keys in seismic behavior of bridges crossing fault-rupture zones. J Bridge Eng-ASCE 2008;13(4):398–408. https://doi.org/10.1061/(ASCE)1084-0702(2008)13:4(398).
[43] Goel RK, Chopra AK. Linear analysis of ordinary bridges crossing fault-rupture zones. J Bridge Eng-ASCE 2009;14(3):203–15. https://doi.org/10.1061/(ASCE)1084-0702(2009)14:3(203).
[44] Goel RK, Chopra AK. Nonlinear analysis of ordinary bridges crossing fault-rupture zones. J Bridge Eng-ASCE 2009;14(3):216–24. https://doi.org/10.1061/(ASCE)1084-0702(2009)14:3(216).
[45] Guney D, Acar M, Ozludemir MT, Celik RN. Investigation of post-earthquake displacements in viaducts using geodetic and finite element methods. Nat Hazards Earth Syst Sci 2010;10(12):2579–87.
[46] Han Q, Du X, Liu J, Li Z, Li L, Zhao J. Seismic damage of highway bridges during the 2008 Wenchuan earthquake. Earthq Eng Eng Vib 2009;8(2):263–73.
[47] Hanks TC, Bakun WH. A bilinear source-scaling model for M-log *A* observations of continental earthquakes. Bull Seismol Soc Am 2002;92(5):1841–6.
[48] Hanks TC, Bakun WH. M-log *A* observations of recent large earthquakes. Bull Seismol Soc Am 2008;98(1):490–4.
[49] Holzer TL, Barka AA, Carver D, Celebi M, Cranswick E, Dawson T, et al. Implications for earthquake risk prediction in the United States from the Kocaeli, Turkey, earthquake of August 17, 1999. Reston, VA: U.S. Geological Survey Circular 1193; 2000.
[50] Hsu YT, Fu CC. Study of damaged Wushi Bridge in Taiwan earthquake. Pract Period Struct Des Constr-ASCE 2000;5(4):166–71. https://doi.org/10.1061/(ASCE)1084-0680(2000)5:4(166).
[51] Hu S, Yang H-Z, Luo S-B, Wu J-W, Sun P-K. Overall design of Puqian Bridge in Hainan. Bridge Constr 2016;46(1):94–9. [in Chinese].
[52] Huang Y, Wang J, Jin D. Performance of a rigid frame arch bridge under near-fault earthquake ground motion. Adv Mater Res 2011;250–253:1869–72.
[53] Hui Y. Study on ground motion input and seismic response of bridges crossing active fault [Ph.D. Dissertation]. Nanjing, China: School of Transportation, Southeast University; 2015. [in Chinese].
[54] Hui Y, Wang K, Li C. Mechanism of seismic damage and enlightenment seismic design of bridges crossing fault. J Highw Transp Res Dev 2015;9(2):54–60. https://doi.org/10.1061/JHTRCQ.0000441.
[55] Huizing JBS, Bialostocki RJ, Armstrong IC, Thornton RW, Wood JH, Willberg GD. Design of the Thorndon overbridge. NZ Eng 1968;23(12):484–504.
[56] Imbsen RA, Roblee CJ, Yashinsky M, Berilgen MM, Toprak S. Impact on highway structures. Earthq Spectra 2000;16(S1):411–35.
[57] Ingham TJ, Rodriguez S, Nader M. Nonlinear analysis of the Vincent Thomas Bridge for seismic retrofit. Comput Struct 1997;64(5/6):1221–38.
[58] Johnson AM, Johnson KM, Durdella J, Sozen M, Gur T. An emendation of elastic rebound theory: main rupture and adjacent belt of right-lateral distortion detected by Viaduct at Kaynash, Turkey 12 November 1999 Duzce earthquake. J Seismol 2002;6(3):329–46.
[59] Johnson N, Ranf RT, Saiidi MS, Sanders D, Eberhard M. Seismic testing of a two-span reinforced concrete bridge. J Bridge Eng-ASCE 2008;13(2):173–82. https://doi.org/10.1061/(ASCE)1084-0702(2008)13:2(173).
[60] Karmakar D, Ray-Chaudhuri S, Shinozuka M. Finite element model development, validation and probabilistic seismic performance evaluation of Vincent Thomas suspension bridge. Struct Infrastruct Eng 2015;11(2):223–37.
[61] Kawashima K. Damage of bridges resulting from fault rupture in the 1999 Kocaeli and Duzce, Turkey earthquakes and the 1999 Chi-Chi, Taiwan earthquake. In: Proceedings of the 1st workshop on seismic fault-induced failures-possible remedies for damage to urban facilities. Tokyo, Japan: University of Tokyo Press; 2001, p. 171–90.
[62] Kawashima K. Damage of bridges resulting from fault rupture in the 1999 Kocaeli and Duzce, Turkey earthquakes and the 1999 Chi-Chi, Taiwan earthquake. Struct Eng/Earthq Eng-JSCE 2002;19(2):179s–97s.
[63] Kawashima K, Takahashi Y, Ge H, Wu Z, Zhang J. Reconnaissance report on damage of bridges in 2008 Wenchuan, China, earthquake. J Earthq Eng 2009;13(7):965–96.
[64] Kelson KI, Bray J, Cluff L, Harder L, Kieffer S, Lettis W, et al. Fault-related surface deformation. Earthq Spectra 2001;17(S1):19–36.
[65] Kelson KI, Koehler RD, Kang K-H, Bray JD, Cluff LS. Surface deformation produced by the 1999 Chi-Chi (Taiwan) earthquake and interactions with built structures, Report to U.S. Geological Survey, NEHRP Award No. 01-HQ-GR-0122. Walnut Creek, CA: William Lettis and Associates, Inc.; 2003.
[66] Konagai K, Kunimatsu S, Ueta K, Uehan F, Onizuka N, Kiku H, et al. Infrastructures near seismic faults, Report of JSPS Research Project No. 16208048. Tokyo, Japan: Japan Geotechnical Society; 2007.
[67] Konakli K, Der Kiureghian A. A response spectrum method for analysis of bridges crossing faults. In: Proceedings of the 2nd international conference on computational methods in structural dynamics and earthquake engineering. Rhodes, Greece; 2009.
[68] Kosa K, Shi Z, Zhang J, Shimizu H. Damage analysis of Xiaoyudong Bridge affected by Wenchuan earthquake, China. J Struct Eng-JSCE 2011;57A:431–41.
[69] Kosa K, Tazaki K, Yamaguchi E. Mechanism of damage to Shiwei Bridge caused by 1999 Chi-Chi earthquake. In: Proceedings of the 1st workshop on seismic fault-induced failures-possible remedies for damage to urban facilities. Tokyo, Japann: University of Tokyo Press; 2001, p. 155–60.
[70] Lawson AC, et al. The California earthquake of April 18, 1906: report of the state earthquake investigation commission. Publication no. 87. I. Washington, DC:

Carnegie Institution of Washington; 1908.
[71] Li H, Lu M, Wen Z, Luo R. Characteristics of bridge damages in Wenchuan earthquake. J Nanjing Univ Technol 2009;31(1):24–9. [in Chinese].
[72] Lin C-CJ, Hung H-H, Liu K-Y, Chai J-F. Reconnaissance observation on bridge damage caused by the 2008 Wenchuan (China) earthquake. Earthq Spectra 2010;26(4):1057–83.
[73] Lin C-T. Images of the 921 great earthquake – 10th anniversary. Geology 2009;28(3):1–32. [in Chinese].
[74] Liu K-Y. Introduction to the 921 Chi-Chi earthquake on-line museum. Arch Q 2010;8(3):132–43. [in Chinese].
[75] Liu Z. Reconnaissance and preliminary observations of bridge damage in the great Wenchuan earthquake, China. Struct Eng Int 2009;19(3):277–82.
[76] Luo Z, Li J. Study on the characteristics of the seismic response of a cable-stayed bridge crossing a fault rupture zone. In: Proceedings of the 2014 national annual conference on highway maintenance technology. Nanjing, China; 2014, p. 175–180. [in Chinese].
[77] Marinos PG, Tsiambaos GT, Kavvadas M. Geological and geotechnical conditions of the Corinth Canal. In: Proceedings of the international symposium on engineering geology and the environment. Athens, Greece; 2001, p. 3987–4003.
[78] Marioni A. Behaviour of large base isolated prestressed concrete bridges during the recent exceptional earthquakes in Turkey. In: Proceedings of the seminar Difendiamoci dai terremoti: le piu recenti applicazioni italiane delle nuove tecnologie antisismiche d'isolamento e dissipazione energetica". Bologna, Italy; 2000.
[79] Matsunaga S, Otsuka H. Seismic performance of a RC arch bridge subjected to fault displacement. J Jpn Soc Civ Eng Ser A1 (Struct Eng Earthq Eng (SE/EE)) 2009;65(1):417–25. [in Japanese].
[80] Maurin P. The Mercureaux Viaduct: study of the foundation of a large bridge built across a major fault lying in the Besancon fault system. Bull Des Lab Des Ponts Chauss- 2001;233:79–88.
[81] Mavroeidis GP, Papageorgiou AS. A mathematical representation of near-fault ground motions. Bull Seismol Soc Am 2003;93(3):1099–131.
[82] Meng J, Liu Z. Causation analysis and enlightenment on bridge unseating in the great Wenchuan earthquake. Struct Eng 2010;26(2):95–100. [in Chinese].
[83] Ministry of Construction of the People's Republic of China (MCPRC) and General Administration of Quality Supervision, Inspection and Quarantine of the People's Republic of China (AQSIQ). Code for seismic design of railway engineering. Beijing, China; 2009. [in Chinese].
[84] Ministry of Housing and Urban-Rural Development of the People's Republic of China (MOHURD). Code for seismic design of urban bridges. Beijing, China; 2011. [in Chinese].
[85] Ministry of Transport of the People's Republic of China (MTPRC). Guidelines for seismic design of highway bridges. Beijing, China; 2008. [in Chinese].
[86] Ministry of Transport of the People's Republic of China (MTPRC). Specification of seismic design for highway engineering. Beijing, China; 2013. [in Chinese].
[87] Mitchell JK, Martin II JR, Olgun CG, Emrem C, Durgunoglu HT, Cetin KO, et al. Performance of improved ground and earth structures. Earthq Spectra 2000;16(S1):191–225.
[88] Mizuguchi T, Abe M, Fujino Y. Modeling and countermeasures for unseating of bridges caused by surface earthquake fault in 1999 Taiwan Chi-Chi earthquake. Doboku Gakkai Ronbunshu 2002;710:257–71. [in Japanese].
[89] Mokha AS, Zayas VA. Seismic isolation retrofit of a 2.3 km long concrete viaduct structure crossing an active fault in Turkey. In: Proceedings of the 6th world congress of joints, bearings and seismic systems for concrete structures. Halifax, Canada; 2006.
[90] Motohashi H, Nonaka T, Magoshi K, Nakamura M, Harada T. Numerical simulation of ground motions and damage of bridge in near field of the 2016 Kumamoto earthquake fault. Kozo Kogaku Ronbunshu A (J Struct Eng A) 2017;63A:339–52. [in Japanese].
[91] Moss RES, Ross ZE. Probabilistic fault displacement hazard analysis for reverse faults. Bull Seismol Soc Am 2011;101(4):1542–53.
[92] Murono Y, Miroku A, Konno K. Experimental study on mechanism of fault-induced damage of bridges. In: Proceedings of the 13th world conference on earthquake engineering. Vancouver, Canada; 2004, Paper No. 1132.
[93] National Center for Research on Earthquake Engineering (NCREE). Preliminary report on the damage of the 921 Chi-Chi earthquake, Report No. NCREE-99-033. Taipei, Taiwan; 1999. [in Chinese].
[94] New Zealand Transport Agency (NZTA). Bridge manual, 3rd edition. Wellington, New Zealand; 2016.
[95] OpenSees. 〈http://opensees.berkeley.edu/〉, [Mar. 13, 2018].
[96] Otsuka H, Nakamura T, Furukawa A. Seismic safety of a steel cable-stayed bridge subjected to fault displacement. Kozo Kogaku Ronbunshu A (J Struct Eng A) 2009;55A:593–604. [in Japanese].
[97] Pamuk A, Kalkan E, Ling HI. Structural and geotechnical impacts of surface rupture on highway structures during recent earthquakes in Turkey. Soil Dyn Earthq Eng 2005;25(7):581–9.
[98] Park SW, Ghasemi H, Shen J, Somerville PG, Yen WP, Yashinsky M. Simulation of the seismic performance of the Bolu Viaduct subjected to near-fault ground motions. Earthq Eng Struct Dyn 2004;33(13):1249–70.
[99] Petersen MD, Dawson TE, Chen R, Cao T, Wills CJ, Schwartz DP, et al. Fault displacement hazard for strike-slip faults. Bull Seismol Soc Am 2011;101(2):805–25.
[100] Priestley MJN, Calvi GM. Strategies for repair and seismic upgrading of Bolu Viaduct 1, Turkey. J Earthq Eng 2002;6(S1):157–84.
[101] Roussis PC, Constantinou MC, Erdik M, Durukal E, Dicleli M. Assessment of performance of seismic isolation system of Bolu Viaduct. J Bridge Eng-ASCE 2003;8(4):182–90. https://doi.org/10.1061/(ASCE)1084-0702(2003)8:4(182).
[102] Saiidi MS, Vosooghi A, Choi H, Somerville P. Shake table studies and analysis of a two-span RC bridge model subjected to a fault rupture. J Bridge Eng-ASCE 2014;19(8):A4014003. https://doi.org/10.1061/(ASCE)BE.1943-5592.0000478.
[103] SAP2000. 〈https://www.csiamerica.com/products/sap2000〉, [Mar. 13, 2000].
[104] Seible F. Long span bridges in California – seismic design and retrofit issues. In: Proceedings of the 12th world conference on earthquake engineering. Auckland, New Zealand; 2000, Paper No. 2614.
[105] Sezen H, Elwood KJ, Whittaker AS, Mosalam KM, Wallace JW, Stanton JF. Structural engineering reconnaissance of the August 17, 1999, Kocaeli (Izmit), Turkey, earthquake, PEER Report No. 2000/09. Berkeley, CA: Pacific Earthquake Engineering Research Center; 2000.
[106] Shantz T, Alameddine F, Simek J, Yashinsky M, Merriam M, Keever M. Evaluation of fault rupture hazard mitigation. In: Proceedings of the 7th national seismic conference on bridges and highways. Oakland, CA; 2013.
[107] Shi Z. Study on seismic behavior and failure mechanism of full scale RC bridges [Ph.D. Dissertation]. Fukuoka, Japan: Department of Civil Engineering, Kyushu Institute of Technology; 2015.
[108] Shi Z, Kosa K, Zhang J, Sasaki T. Damage assessment-based dynamic analysis of a RC rigid-frame arch bridge affected by Wenchuan earthquake. J Struct Eng-JSCE 2013;59A:459–71.
[109] Shirahama Y, Yoshimi M, Awata Y, Maruyama T, Azuma T, Miyashita Y, et al. Characteristics of the surface ruptures associated with the 2016 Kumamoto earthquake sequence, central Kyushu, Japan. Earth Planets Space 2016;68:191. https://doi.org/10.1186/s40623-016-0559-1.
[110] Shuai S, Dai W, Luo S. Study on the design of bridges crossing fault rupture zones. Highway 2016;4:127–30. [in Chinese].
[111] Slemmons DB, dePolo CM. Chapter 3: evaluation of active faulting and associated hazards. In: Wallace RE, editor. Studies in geophysics: active tectonic. Washington, DC: National Academy Press; 1986. p. 45–62.
[112] Slemmons DB, McKinney R. Definition of "active fault". Miscellaneous Paper S-77-8. Vicksburg, MS: U.S. Army Engineer Waterways Experiment Station; 1977.
[113] Smyth AW, Pei J-S, Masri SF. System identification of the Vincent Thomas suspension bridge using earthquake records. Earthq Eng Struct Dyn 2003;32(3):339–67.
[114] Sojourner A, Ostrom TA, Shantz TJ, Yashinsky M. Addressing fault rupture hazard for bridges across California. In: Proceedings of the 110th annual meeting of the seismological society of America. Pasadena, CA [Abstract in Seismological Research Letters 86(2B), 702–3]; 2015.
[115] Stathopoulos S. Chapter 12: bridge engineering in Greece. In: Chen WF, Duan L, editors. Handbook of international bridge engineering. Boca Raton, FL: CRC Press; 2014. p. 481–559.
[116] Su S, Li S, Hao L, Mei H. Characteristics and mechanism of deformation and failure of Xiaoyudong Bridge caused by Wenchuan earthquake. J Catastrophol 2011;26(4):19–23. [in Chinese].
[117] Sung Y-C, Chang K-C, Chang D-W, Hung H-H, Liu K-Y. Damage investigation and seismic retrofit of bridges in Taiwan after 921 Chi-Chi earthquake. In: Proceedings of the international symposium on engineering lessons learned from the 2011 great east Japan earthquake. Tokyo, Japan; 2012.
[118] Takami T, Yano K, Omata M, Chida K, Tamura H, Hashimoto S, et al. Relationship between damaged bridge and surrounding ground deformation occurred in the 2016 Kumamoto earthquake. 〈http://www.jseg.or.jp/00-main/pdf/20161109_takami.pdf〉, [Mar. 10, 2018, in Japanese].
[119] Tasaki K, Kosa K, Yamaguchi E, Shoji G. Damage analysis of a bridge affected by the Chi-Chi earthquake. Doboku Gakkai Ronbunshu 2005;794:143–56. [in Japanese].
[120] Thatcher W, Lisowski M. Long-term seismic potential of the San Andreas fault southeast of San Francisco, California. J Geophys Res 1987;92(B6):4771–84.
[121] Todorovska MI, Trifunac MD. Selection of comprehensive design criteria for highway bridges in the vicinity of and crossing active faults, Report to METRANS Transportation Center, Project 07-24. Los Angeles, CA: University of Southern California; 2013.
[122] Tokida K. Simplified procedure to estimate relative displacement of bridge and embankment induced by surface faulting. In: Proceedings of the 27th JSCE earthquake engineering symposium. Japan; 2003. [in Japanese].
[123] Tokida K, Watanabe T, Hiraishi H. Countermeasures for a highway bridge against an active surface fault displacement. In: Proceedings of the 28th JSCE earthquake engineering symposium. Japan; 2005. [in Japanese].
[124] Ucak A, Mavroeidis GP, Tsopelas P. Behavior of a seismically isolated bridge crossing a fault rupture zone. Soil Dyn Earthq Eng 2014;57:164–78.
[125] Uckan E, Oven VA, Erdik M. A study of the response of the Mustafa Inan Viaduct to the Kocaeli earthquake. Bull Seismol Soc Am 2002;92(1):483–98.
[126] Ulusay R, Aydan O, Hamada M. The behavior of structures built on active fault zones: examples from the recent earthquakes of Turkey. In: Proceedings of the 1st workshop on seismic fault-induced failures-possible remedies for damage to urban facilities. Tokyo, Japan: University of Tokyo Press; 2001, p. 1–26.
[127] Unjoh S, Kondoh M. Analytical study on the effect of fault displacement on the seismic performance of bridge structures. In: Proceedings of the 2nd international workshop on mitigation of seismic effects on transportation structures. Taipei, Taiwan: National Center for Research on Earthquake Engineering; 2000, p. 222–33.
[128] Uzuoka R. Section 2.4: infrastructure damage. In: Report on the Chi-Chi, Taiwan earthquake of september 21, 1999, EDM Technical Report No. 7, Miki, Japan: Earthquake Disaster Mitigation Research Center; 2000, p. 42–51.
[129] Wallace JW, Eberhard MO, Hwang S-J, Moehle JP, Post T, Roblee C, et al. Highway bridges. Earthq Spectra 2001;17(S1):131–52.
[130] Wang D, Guo X, Sun Z, Meng Q, Yu D, Li X. Damage to highway bridges during Wenchuan earthquake. Earthq Eng Eng Vib 2009;29(3):84–94. [in Chinese].

[131] Wang Z. A preliminary report on the Great Wenchuan earthquake. Earthq Eng Eng Vib 2008;7(2):225–34.
[132] Wang Z, Lee GC. A comparative study of bridge damage due to the Wenchuan, Northridge, Loma Prieta and San Fernando earthquakes. Earthq Eng Eng Vib 2009;8(2):251–61.
[133] Wells DL, Coppersmith KJ. New empirical relationships among magnitude, rupture length, rupture width, rupture area, and surface displacement. Bull Seismol Soc Am 1994;84(4):974–1002.
[134] Willis B. A fault map of California. Bull Seismol Soc Am 1923;13(1):1–12.
[135] Wong RHC, Zhang Q-B, Cheung KHT. Geotechnical model testing of surface rupture and bridge damage produced by discontinuous reverse faults. J Sichuan Univ (Eng Sci Ed) 2010;42(5):58–67. [in Chinese].
[136] Wood J. Strong motion records from the Thorndon Overbridge in the 2013 Cook Strait and Lake Grassmere earthquakes. In: Proceedings of the annual conference of the New Zealand society of earthquake engineering. Auckland, New Zealand; 2014, Paper No. O77.
[137] Wu SL, Charatpangoon B, Kiyono J, Maeda Y, Nakatani T, Li SY. Near-fault ground displacement for seimic design of bridge structures. In: Proceedings of the 16th world conference on earthquake engineering. Santiago, Chile; 2017, Paper No. 1490.
[138] Xu J, Liu X. Study on bridge collapse resulting from fault rupture. China Railw Sci 2008;29(1):17–21. [in Chinese].
[139] Xu Z, Wang S, Lin Z. Discussion of damage modes of bridges and roadways in the 921 great earthquake. In: Proceedings of the 9th Guangdong-Hong Kong-Macau-Taiwan engineers forum. Guangzhou, China; 2011, p. 140–50. [in Chinese].
[140] Yang H, Li J. Response analysis of seismic isolated bridge under influence of fault-crossing ground motions. J Tongji Univ (Nat Sci) 2015;43(8):1144–52. [in Chinese].
[141] Yang S, Mavroeidis GP, Ucak A, Tsopelas P. Effect of ground motion filtering on the dynamic response of a seismically isolated bridge with and without fault crossing considerations. Soil Dyn Earthq Eng 2017;92:183–91.
[142] Yashinsky M. Chapter 7: highway systems. In: Chi-Chi, Taiwan, earthquake of september 21, 1999: lifeline performance, technical council on lifeline earthquake engineering. Reston, VA: American Society of Civil Engineers, Monograph No. 18; 2000, p. 119–77.
[143] Yashinsky M, Ostrom T. Caltrans' new seismic design criteria for bridges. Earthq Spectra 2000;16(1):285–307.
[144] Yen W-H. Lessons learned about bridges from earthquake in Taiwan. Public Roads 2002;65(4):20–3.
[145] Yen WP, Chen G, Yashinsky M, Hashash Y, Holub C, Wang K, et al. Bridge lessons learned from the Wenchuan, China, earthquake. Transp Res Rec: J Transp Res Board 2010;2202:102–8.
[146] Yen W-HP, Chen G, Yashinsky M, Hashash Y, Holub C, Wang K, et al. China earthquake reconnaissance report: performance of transportation structures during the May 12, 2008, M7.9 Wenchuan earthquake. Publication No. FHWA-HRT-11-029. Washington, DC: Federal Highway Administration; 2011.
[147] Yuan Y, Sun B, et al. General introduction of engineering damage of Wenchuan Ms 8.0 earthquake. Earthq Eng Eng Vib 2008;28(Supplement):S1–114.
[148] Zeng Y. Study on the nonlinear dynamic response and damage feature of cable-stayed bridge in deep water excited by cross-fault earthquakes [Master Thesis]. Beijing, China: Department of Civil Engineering, Beijing Jiaotong University; 2016. [in Chinese].
[149] Zhao B, Taucer F. Performance of infrastructure during the May 12, 2008 Wenchuan earthquake in China. J Earthq Eng 2010;14(4):578–600.
[150] Zhou G, Cui C, Liu B, Li X. Failure modes of near-fault bridges in Wenchuan earthquake. Technol Earthq Disaster Prev 2008;3(4):370–8. [in Chinese].
[151] Zhu B, Cui S, Yu M. Analysis of seismic failure on Xiaoyudong Bridge across fault zone in Wenchuan earthquake. J Highw Transp Res Dev 2010;27(1):78–83. [in Chinese].
[152] Zhuang W, Liu Z, Jiang J. Earthquake-induced damage analysis of highway bridges in Wenchuan earthquake and countermeasures. Chin J Rock Mech Eng 2009;28(7):1377–87. [in Chinese].